New information on ornithopod dinosaurs from the Late Jurassic of Portugal

FILIPPO MARIA ROTATORI, MIGUEL MORENO-AZANZA, and OCTÁVIO MATEUS

Rotatori, F.M., Moreno-Azanza, M., and Octávio, M. 2020. New information on ornithopod dinosaurs from the Late Jurassic of Portugal. *Acta Palaeontologica Polonica* 65 (1): 35–57.

Ornithopods are one of the most speciose group of herbivorous dinosaurs, rising during the Jurassic and getting extinct at the Cretaceous–Paleogene boundary. However, most of the attention has been given to derived forms (hadrosaurids). Herein, cranial and post-cranial ornithopod material from the Upper Jurassic Lourinhã Formation and housed at Museu da Lourinhã is described and discussed. Comparison and phylogenetic analyses has allowed the attribution of the material either to Dryosauridae or to Ankylopollexia. The large-sized taxa conservatively ascribed to Ankylopollexia, resemble more closely Early Cretaceous styracosternans than Late Jurassic taxa. Due to the lack of autapomorphic characters, it was not possible to assign the material to any of the two valid Jurassic ornithopod Portuguese species, *Draconyx loureiroi* and *Eousdryosaurus nanohallucis*, although phylogenetic analyses hint a close relationship between the Lourinhã dryosaurid material and *E. nanohallucis*. Principal Component Analysis plotting limb bones proportions indicates a not fully mature ontogenetic stage for the Portuguese specimens. Comparing the Portuguese ornithopod fauna with the one in Morrison Formation and Kimmeridge Clay Formation, it is remarked the key-role of Portugal to understand biogeographic patterns in the distribution of iguanodontians.

Key words: Dinosauria, Ornithischia, Iguanodontia, taxonomy, systematics, biogeograhy, Jurassic, Lourinhã Formation, Portugal.

Filippo Maria Rotatori [filippo.rotatori.93@gmail.com], Miguel Moreno-Azanza [mmazanza@gmail.com], and Octávio Mateus [omateus@fct.unl.pt], GeoBioTec, Department of Earth Sciences, Faculdade de Ciências e Tecnologia, FCT, Universidade Nova de Lisboa, 2829-516 Caparica, Portugal; Museu da Lourinhã, Espaço Novapaleo, Rua João Luis de Moura 95, 2530-158 Lourinhã, Portugal.

Received 5 August 2019, accepted 4 December 2019, available online 4 March 2020.

Introduction

Ornithopods are among the most successful groups of dinosaurs from the Mesozoic. They range from the Jurassic (Ruiz-Omeñaca et al. 2006) to the end of the Cretaceous (Horner et al. 2004). Ornithopoda contains some iconic species and some of the very first taxa known to paleontology (Horner et al. 2004; Norman 2004). Systematic studies with cladistic approaches on the Ornithopoda began in the 1980s (Norman 1984; Sereno 1984, 1986) and for a long time the relationships within the clade remained stable. However, in recent years, many systematic revisions challenged the very first phylogenetic hypothesis (Butler et al. 2008; Boyd 2015; Madzia et al. 2018). These revisions affected primarily the base of Ornithopoda (non-iguanodontian ornithopods), while more derived taxa maintained stable positions. Jurassic basal iguanodontians are a rare component of terrestrial faunal assemblages (Foster 2007). The majority of the taxa and specimens are known from the North American Morrison Formation, and from the Tanzanian Tendaguru Formation (Gilmore 1909; Janensch 1955; Galton 1981; Carpenter and Wilson 2008; McDonald 2011), while European faunas are far less abundant. From Portugal, the Guimarota Mine lignites yielded a rich fossiliferous assemblage, providing significant insights on the structure of Late Jurassic ecosystems (Martin and Krebs 2000). Among the dinosaurian fauna, in 1973 Thulborn erected the species *Phyllodon henkeli*, a small ornithischian which appears to be closely related to *Drinker nisti* and *Othnielosaurus rex* from the Morrison Formation (Martin and Krebs 2000). Rauhut (2001) described a large sample of herbivorous dinosaur material from Guimarota, reporting on over 100 teeth and a fragmentary dentary ascribed to *Phyllodon*, and proposed a diagnosis of the species based on the arrangement and proportion of the tooth ridges. In addition, Rauhut (2001) reported three dentary teeth ascribed to indeterminate iguanodontians. From the Upper Callovian locality of Pedrógao, in Leiria

municipality, Thulborn (1973) erected the taxon *Alocodon kuehnei* based on isolated teeth. Most of the Late Jurassic ornithischians of Portugal come from the outcrops of the Lourinhã Formation (Antunes and Mateus 2003) including *Trimucrodon cuneatus* and cf. *Hypsilophodon* from the Porto Dinheiro locality (Thulborn 1973). Due to the fragmented state of the specimens and the paucity of subsequent discoveries, a clear assessment of this material is problematic (Norman et al. 2004). Two undisputed iguanodontian species were recovered from Lourinhã Formation: the camptosaurid *Draconyx loureiroi* (Mateus and Antunes 2001) and the dryosaurid *Eousdryosaurus nanohallucis* (Escaso et al. 2014). The holotypes consist of fragmentary post-cranial elements. *D. loureiroi* has been treated as a wildcard in several phylogenetic analyses dealing with basal iguanodontians relationships (McDonald 2012; Boyd 2015), while *E. nanohallucis* is represented by an immature individual (Escaso et al. 2014). The scarcity of ornithopod and, in general, neornithischian remains, strongly contrasts with the abundance of other herbivorous dinosaurs, such as sauropods and thyreophorans (Antunes and Mateus 2003). Up until now it has not been possible to assess if this gap may be due to differential preservation linked to ecological segregation as seen for ornithischians and saurischians in the Morrison Formation (Foster 2013) or if it reflects inter-specific competition between different herbivorous taxa. Beside skeletal and dental ornithopod fossils, various tracks and track-sites have been reported from the Lourinhã Formation (Mateus and Milàn 2009) including a giant sized *Iguanodontipus*-like footprint which is 70 cm long, suggesting the presence of a large sized iguanodontian possibly larger than any previously known Late Jurassic species (Mateus and Milàn 2008), but also smaller sized camptosaurid tracks (as figured by Antunes and Mateus 2003: fig. 11) and *Dinehichnus*-like ones, probably made by dryosaurids or other small bipedal neornithischians (Mateus and Milàn 2009).

Here, we extend the current knowledge of the Late Jurassic ornithopod fauna of Portugal, reporting and describing previously unpublished fossils housed at the Museu da Lourinhã.

Institutional abbreviations.—CM, Carnegie Museum of Natural History, Pittsburgh, PA, USA; IRSNB, Institut Royal des Sciences Naturelles de Belgique, Brussels, Belgium; NHMUK, Natural History Museum, London, UK; OUM, Oxford University Museum, Oxford, UK; ML, Museu da Lourinhã, Portugal; SHN, Sociedade de Història Natural, Torres Vedras, Portugal; YPM, Yale Peabody Museum, New Haven, CT, USA; UMNH, Utah Museum of Natural History, Salt Lake City, UT, USA.

Other abbreviations.—CI, consistency index; GM, geometric mean; PCA, Principal Component Analysis; RI, retention index; RMA, Reduced Major Axis; TL,tree length.

Geological settings

Specimens described here were recovered along the coastline in the Lourinhã municipality, western-central Portugal, from a north-south transect that goes from north Vale Pombas to Santa Rita municipality (Fig. 1). All specimens come from the famous and highly fossiliferous Upper Jurassic Lourinhã Formation (Kimmeridgian–Tithonian; Hill 1989). This lithostratigraphic unit comprises a succession of sandstone and mudstone beds, representing braided fluvial systems, alluvial fans and upper deltas, with the occasional presence of shallow marine limestone that represent short transgressive events. The subdivision of the Lourinhã Formation into subunits has been subjected to various revisions (Hill 1989; Manuppella 1998; Manuppella et al. 1999; Taylor et al. 2014). In the present work, we follow the subdivision proposed by Mateus et al. (2017). From bottom to top, the beds outcropping belong to the following members: Porto Novo/Praia de Amoreira, Praia Azul, Santa Rita.

Porto Novo/Praia da Amoreira Member is characterized by a percentage of sands that range 34–44%, and are formed of fluvial channel deposits and calcrete-bearing floodplain mud with occasional fine sand lenses. The depositional environment is interpreted as either distal mudflat of an alluvial fan, or of a braided river system. It is dated to the uppermost Kimmeridgian (Fig. 1) (Hill 1989; Taylor et al. 2014; Mateus et al. 2017).

Praia Azul Member is characterized by a lower percentage of sand with respect to the underlying Porto Novo/Praia da Amoreira Member, ranging 12–25%. Three extensive carbonated shell layers, representing three marine transgression events, can be correlated along the whole basin, being important marker beds (Hill 1989). This member is dated to the Kimmeridgian–Tithonian interval, being the boundary between these two stages corresponding to the second carbonated layer (Hill 1989; Taylor et al. 2014; Mateus et al. 2017).

Santa Rita Member is constituted mainly of mudstone with numerous pedogenic carbonated concretions, intercalated by levels of cross-bedded sandstone. The sandstone elements include large scale point bars, flat tabular lenses, crevasse splay, and levees bodies. This is the youngest member, being dated to Tithonian (Mateus et al. 2017).

Material and methods

Here we report and describe material currently housed at the ML. The specimens were collected in annual field campaigns of the museum during the last two to three decades or donated to the institution by amateurs. Most of the latter lack detailed geological setting and sometimes even geographical location other than just the beach from where they were collected. A detailed analysis of the accompanying notations, remains of the matrix sediment the material, and studying the geological mapping of the referred localities

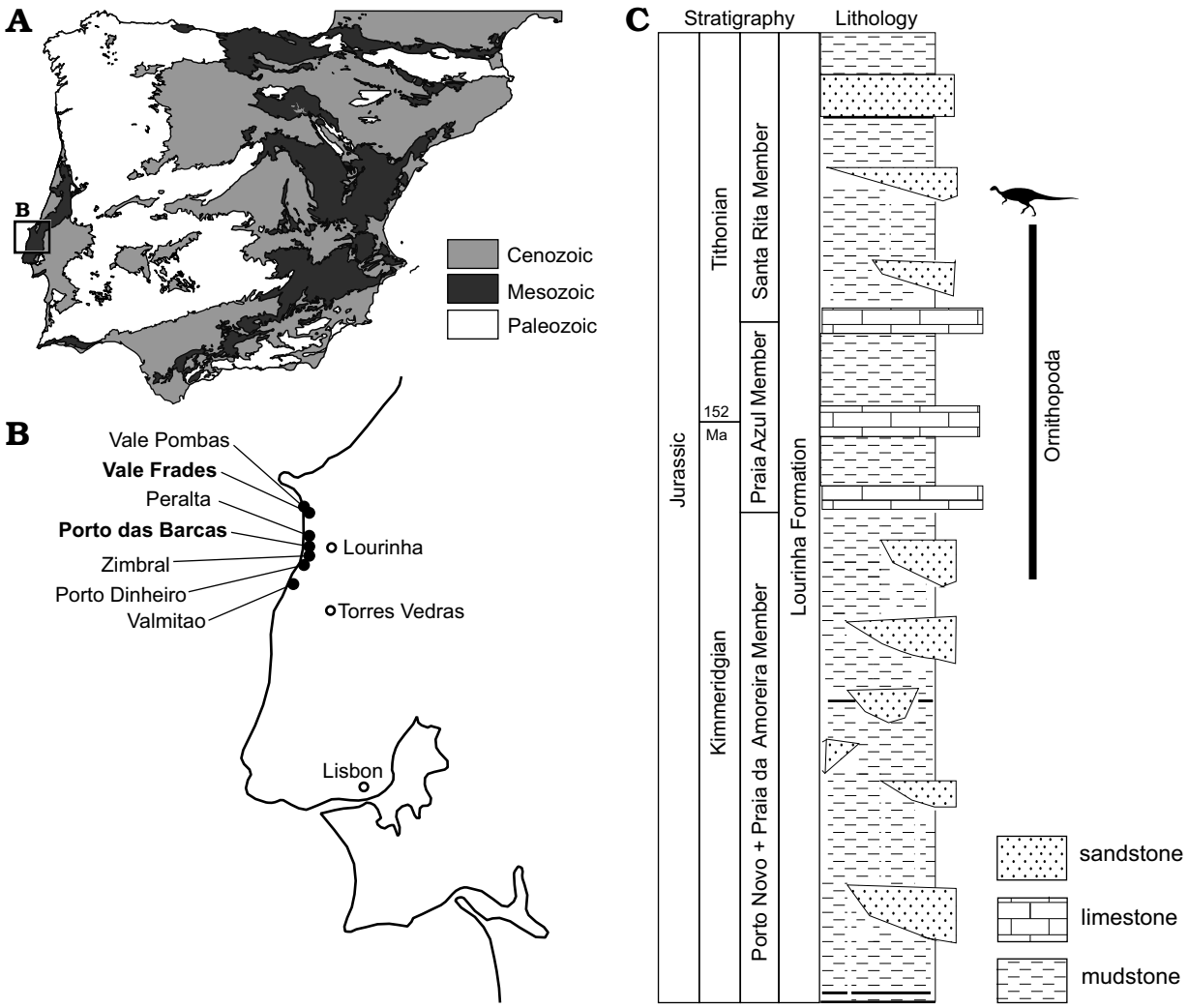

Fig. 1. General map of Iberian Peninsula (**A**), and a close-up of the Lourinhã coastline (**B**), describing the general sedimentology of the Lourinhã Formation and the stratigraphic distribution of the material here discussed (**C**). The localities indicated represent the geographical provenance of the specimens. The type localities of *Draconyx loureiroi* and *Eousdryosaurus nanohallucis* marked in bold. Credit for the Iberian Peninsula map: Eduardo Puértolas-Pascual.

has allowed us to refer most of the material to Praia Azul Member, although at the present time is not possible to determine if it is latest Kimmeridgian or earliest Tithonian in age. ML 2206 comes from the Santa Rita Member and it can be considered to be Early Tithonian in age. ML 563 has no precise information regarding its provenance. Nomenclature follows Galton (1981, 1983), Weishampel (1984) and Norman (1980, 1986). Further photographic comparison was carried out using photographic material including *Dryosaurus*: CM 3392, CM 11340, CM 21786, NHM 723, NHM 724, NHM 725, NMNHUK 812.

In order to assess their phylogenetic relationships, ML 768, ML 2055, ML 563, and ML 818 were included in the matrix of Dieudonné et al. (2016). Despite the topology of the consensus, Dieudonné et al. (2016) differs from the latest studies on the relations of some important clades (Herne et al. 2019; Rozadilla et al. 2019), it is still the best phylogeny to explore the relations of basal ornithopods, including dryosaurids. All character numbers and scores used in the description refers to this dataset. The holotype of *Eousdryosaurus nanohallucis* (SHN 177) was added to the dataset. A heuristic search of 1000 replicates holding 10 trees per replicate was performed for each of the multiple analyses conducted. The analyses were carried out in TnT, version 1.5. (Goloboff and Catalano 2016). The complete data matrix used in the phylogenetic analysis is in SOM 1, and the complete analyses consensus trees are in SOM 2 (Supplementary Online Material available at http://app.pan.pl/SOM/app65-Rotatori_etal_SOM.pdf). In order to reinforce our results, the ML 768, ML 818, ML 2055, and ML 563 were scored in the dataset of Boyd (2015), with the modifications of Madzia et al. (2018) and Bell et al. (2018). Three additional analyses were performed, using the same tree search strategy as in the previous case. The two isolated dentaries (ML 818, ML 768) were run separately (CI 0.344, RI 0.643, TL 914, CI 0.344, RI 0.644, TL 914, respectively), while limb bones elements (ML 563, ML 2055) were run together (CI 0.343, RI 0.642, TL 916). In order to improve the resolution of the results, nine wild-card taxa were individuated using the TnT function pcrprune. We safely removed

Table 1. Selected measurements (in mm) of the specimens here described.

		Total length	Width (proximal epiphysis)		Width (distal epiphysis)	
			mediolateral	anteroposterior	mediolateral	anteroposterior
Femora	ML 2055	250	46	43	55	47
	ML 563	188	26.7	27.3	35.2	41.4
Tibiae	ML 2055	220	40	19	12	30
	ML 505	235	29	44	37	17

		Total length	Width	Height		Thickness (mediolateral)
				max	min	
Dentaries	ML 818	150	–	62	49	23
	ML 768	30	–	7	2	8
Parietal	ML 1851	18	22	–		–
Coracoid	ML 2206	130	108	–		–
Neural arches	ML 2321 (complete)	–	51	22		–
	ML 2321 (partial)	–	35	19		–

		Neural spine		Anterior surface		Posterior surface		Length	
		height	width	height	width	height	width	anteroposterior	transverse process
Isolated dorsal vertebrae	ML 864	140	65	–	–	–	–	75	85
	ML 452	150	50	60	65	65	75	60	90
	ML 452 (incomplete)	–	–	65	73	70	70	65	90

		Total length	Width (min)	Width (distal epiphysis)
Scapula	ML 2042	440	95	120

a posteriori the following taxa: *Burianosaurus augustai*, *Gasparinisaura cincosaltensis*, *Laellynasaura amicagraphica*, *Micropachycephalosaurus hogtuyanensis*, *Morrosaurus antarticus*, *Qantassasaurus intrepidus*, *Stenopelyx valdensis*, and *Weewarrasaurus pobeni*. The results of these new analyses are shown in SOM 3 and SOM 4. Since the obtained results do not provide any particular deeper insight respect to the ones obtained with the matrix of Dieudonné et al. (2016), just the latter ones are discussed in detail here.

The dryosaurids *Dysalotosaurus* and *Dryosaurus* are represented in the fossil record generally by immature specimens (Horner et al. 2009; Hübner 2012, 2018), and that has been proposed to be a distinctive trait of their life history (Hübner 2012). It is still not clear if this trait is common to all dryosaurids, or just to *Dysalatosaurus* and *Dryosaurus*. Recently Hübner (2018) estimated ontogenetic allometric variation in the post-cranial skeleton in a population of the dryosaurid *Dysalotosaurus lettowvorbecki*, based on a linear morphometric approach. In order to test if the limb bones elements ML 2055, ML 563, and ML 505 fitted the model proposed by Hübner (2018), Multivariate Analysis was performed in two steps: PCA and subsequently RMA regression. PCA was embodied to explore the variation between ML specimens and the reference population according to the method described by Hammer and Harper (2008); while RMA was used to extrapolate a growth trajectory for *Dysalotosaurus* individuals plus ML specimens, plotting the log of GM of each specimen. Because the growth of the bone is described by a power function, GM is a reliable proxy of absolute size (Klingenberg 1996). The morphometric dataset is constituted by a subset of the one presented by Hübner (2018), including only the variables directly measurable on the specimens for the femora and tibia (see supplementary material in Hübner 2018 for further explanation). This methodological choice was embodied to minimize the impact of missing data on the analysis. Since allometric variation is described by a power function, the data was log-transformed prior PCA to explore morphometric linear relationships of the variables measured (Hammer and Harper 2008). PCA and RMA were calculated with PAST v.3 (Hammer et al. 2001) In particular, the dataset is composed by linear measurements of post-cranial elements. The variates, the values of principal components and the loading scores are shown in SOM 5–9. Descriptive measurements for all the specimens are given in the Table 1.

Systematic palaeontology

Dinosauria Owen, 1842

Ornithischia Seeley, 1887

Ornithopoda Marsh, 1881

Iguanodontia Sereno, 1986

Dryosauridae Milner and Norman, 1984

Dryosauridae indet.

Figs. 2–4.

Material.—ML 1851, an almost complete isolated parietal from Praia da Peralta; ML 2321, two partial associated neural arches from Praia de Porto Dinheiro; ML 768, a

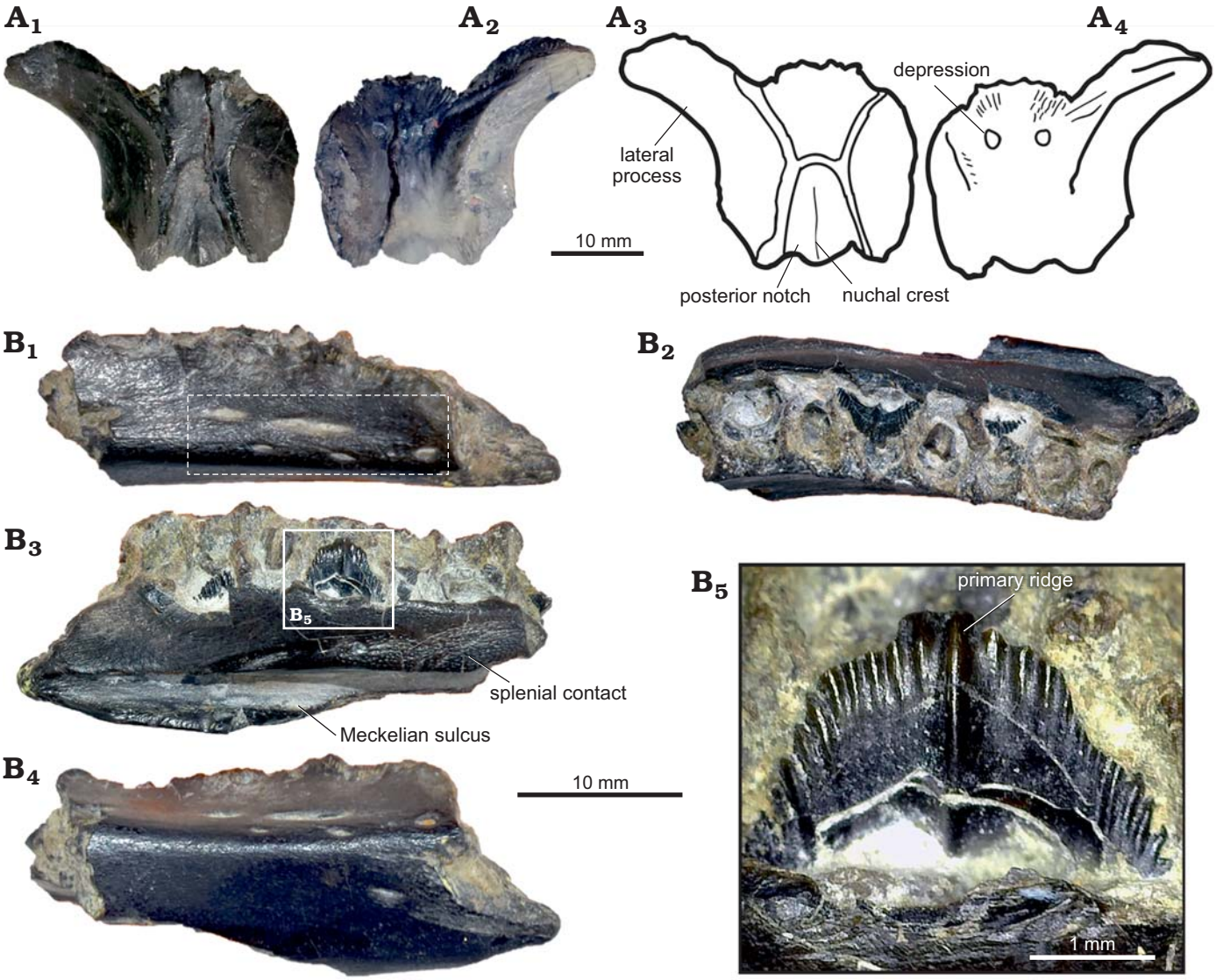

Fig. 2. Cranial material of Dryosauridae indet. from the Lourinhã municipality, Portugal, Lourinhã Formation, Kimmeridgian–Tithonian. **A**. ML 1851, parietal in dorsal (A_1, A_3) and ventral (A_2, A_4) views. **B**. ML 768, dentary in lateral (B_1), dashed frame indicates area with foramina, dorsal (B_2), medial (B_3) and ventral (B_4) views, detail of dentary tooth (B_5).

partial tooth-bearing isolated dentary, ML 2055, associated femur and tibia from Praia do Zimbral; ML 563, isolated femur from Lourinhã coastline; ML 505, isolated tibia from Praia de Vale Pombas. All from Kimmeridgian–Tithonian, Lourinhã, Portugal.

Description.—Cranial skeleton: *Parietal* (Fig. 2A). An isolated almost complete parietal (ML 1851), missing the right lateral half, is 18 mm in length and 22 mm in width. It appears to be sub-triangular in shape, wider anteriorly than posteriorly. The preserved contact with the frontals is W-shaped, presenting an interdigitated suture as seen in *Dysalotosaurus* (Janensch, 1955). The preserved lateral process projects antero-ventrally, having a smooth concave surface. Posteriorly, the lateral processes converge medially to enclose a deep median notch between steep margins. Towards the midline of the notch, the proximal-most part of the nuchal crest is distinguishable although slightly eroded. The ventral surface is concave, flaring in a deep pit anteriorly until the bone margin. Towards the midline pit, two small depressions are preserved.

Dentary (Fig. 2B): ML 768 is a fragment of a right dentary bone (length 30 mm, height 7 mm, latero-medial thickness 8 mm), fractured on both caudal and rostral ends, first reported by Mateus (2006) as aff. *Dryosaurus* sp. It preserves seven tooth positions and one isolated tooth, two erupting teeth and six roots of already worn down teeth. The alveoli display an intra-alveolar border (character 136: 0), but the close proximity of the preserved crowns indicates the absence of intracrown spaces (character 154: 1). In dorsal view, ML 768 is sinuous in shape and the medio-lateral section is slightly concave-convex, towards the lateral surface. The tooth row is convergent anteriorly and divergent posteriorly (character 122: 1). The lateral surface is smooth, bearing seven visible vascular foramina on three different levels

(character 145: 0). On the medial surface, a deep Meckelian sulcus runs for the entire length of the tooth-row. The margins of the sulcus are neat and straight. Caudally, on the medial surface, and dorsal to the Meckelian sulcus, the splenial sutural contact is preserved and it exhibits a highly dense capillary vascular system. The ventral surface does not possess a ventral flange (character 121: 0). The two preserved crowns are diamond-shaped (character 155: 1) and mesiodistally expanded (character 135: 1) with a smoothly rounded apex. The enamel is asymmetrically distributed (character 140: 1), being present only on the lingual surface of the crown. The crown margin possesses coarsely serrated hook-like non-mammilated denticles (character 139: 1). On the lingual side of the crown, an apicobasally extended primary ridge (character 158: 1) is slightly distally offset (character 156: 1), being surrounded by faint secondary ridges (characters 141: 1, 159: 2). The ridges on the enamel are restricted to the lingual surface of the crown (character 160: 1). The denticles are generally not confluent with the crown ridges (character 142: 0), which are less than 10 in number (character 157: 0). The worn down remains of dentary teeth (character 137: 1) do not show the presence of a cingulum between the crown and the root (character 143: 1).

Axial skeleton: *Neural arches* (Fig. 3): Two small associated disarticulated neural arches (ML 2321) appear to be fractured and subsequently restored. One is almost complete, preserving both transverse processes (height 22 mm, width 51 mm) and missing part of the neural canal. The other element preserves just the right transverse process (height 19 mm, width 35 mm). Both specimens show a low degree of distortion, due to taphonomic processes. The neural spine is low and blade like, as is common in vertebrae of other basal iguanodontians from the cervical or anterior-dorsal series (Norman 2004). Anteriorly, two slender and lobed prezygapophyses are present, positioned at about 45° relative to the horizontal. There is a well-marked constriction between the lobe located on the anterior-most end of the prezygapophyses, and the rest of the bony process. Posteriorly to the prezygapophyses, the prezygapophyseal lamina and the anterior centroparapophyseal lamina form a small notch. On the transverse processes, the diapophyses are broken towards the distal edge, showing a sub-triangular transverse section. The parapophyses, located ventrally to the diapophyses shaft, are constrained in the proximal half of the transverse process. Ventral to the parapophyses, on the lateral sides of the neural arches, a shallow depression is present. The two postzygapophyses, lobed like the prezygapophyses, show the same degree of inclination with respect to the horizontal. On the posterior side, wider and deeper notches, in comparison to the notches present on the anterior side, are formed by the postzygodiapophyseal lamina, posterior centrodiapophyseal lamina and centropostzygapophyseal lamina. The same structure is seen in *Valdosaurus* (Barrett et al. 2011). Ventrally, the two lateral walls of the neural canal, present a rugose surface, indicating an incomplete fused condition.

Appendicular skeleton: *Femora* (Fig. 4A, B): The left femur ML 563 is fragmented and heavily distorted. The proximal and distal ends are slightly eroded and fractured. Another, less distorted right femur (ML 2055) measures 250 mm in total length. In ML 563 the general outline of the femoral shaft is strongly bowed anteriorly (character 248: 0). The proximal epiphysis partially preserves the femoral head, which is separated posteriorly by a shallow depression (inter-trochanteric fossa) from the greater trochanter (character 249: 1). The surface of the greater trochanter is flattened (character 252: 1). A broken blade-like surface, which represents the base of the 4th trochanter, is located in the proximal half of the shaft (character 254: 0). Medially, a collapsed surface overlaps the scar of the insertion of Musculus caudofemoralis longus, which is restricted to the medial surface of the shaft (character 256: 1). The distal epiphysis includes both condyles, with the medial larger than the lateral. The two condyles are divided anteriorly by a shallow, V-shaped extensor intercondylar groove (characters 257: 1, 258: 0) and posteriorly by a deep flexor grove. A small lateral process overhangs on the flexor groove opening (character 259: 1). The medial condyle is square shaped and straight, while the lateral presents a slightly inclined anterior edge, and a conspicuous finger-like posterior process (character 260: 1). The medial condyle protrudes cranially towards the lateral condyle (character 261: 1).

As in ML 563, ML 2055 presents the femoral shaft is bowed anteriorly (character 248: 0), being thick and robust in general proportions. The section is sub-triangular in the proximal and mid part of the shaft, becoming more rounded towards the distal epiphysis. The proximal epiphyisis preserves part of the femoral head with a constriction between it and the greater trochanter (character 249: 1). What is preserved of the greater trochanter shows a slightly convex surface (character 252: 0). On the medial surface of the shaft, positioned towards the mid-shaft but slightly proximal (character 254: 0), is a blade, like 4th trochanter (characters 253: 1, 255: 0) that is directed medioventrally. The scar of the Musculus caudofemoralis longus extends more to the base of the trochanter with respect to ML 563, but is still separated from it (character 256: 1). Distally, the epiphysis has both condyles preserved, divided anteriorly by a very prominent U-shaped extensor groove (character 257: 1, 258: 0). This groove is proportionally deeper than in ML 563. Posteriorly, the two condyles are separated by a deeper, fully open, flexor groove (character 259: 0). As in ML 563, the posterior finger-like process of the lateral condyle is strongly inset (character 260: 1), whereas medial condyle does not protrude cranially to the lateral condyle (character 261: 0).

Tibiae (Fig. 4C, D): Two partially preserved right tibiae, present various degrees of erosion and fracturing. The specimen ML 505 is a heavily eroded but complete right tibia with some longitudinal fractures along the proximal and distal epiphyses. It measures 235 mm in total length. The tibia ML 2055, associated with the ML 2055 femur, lacks

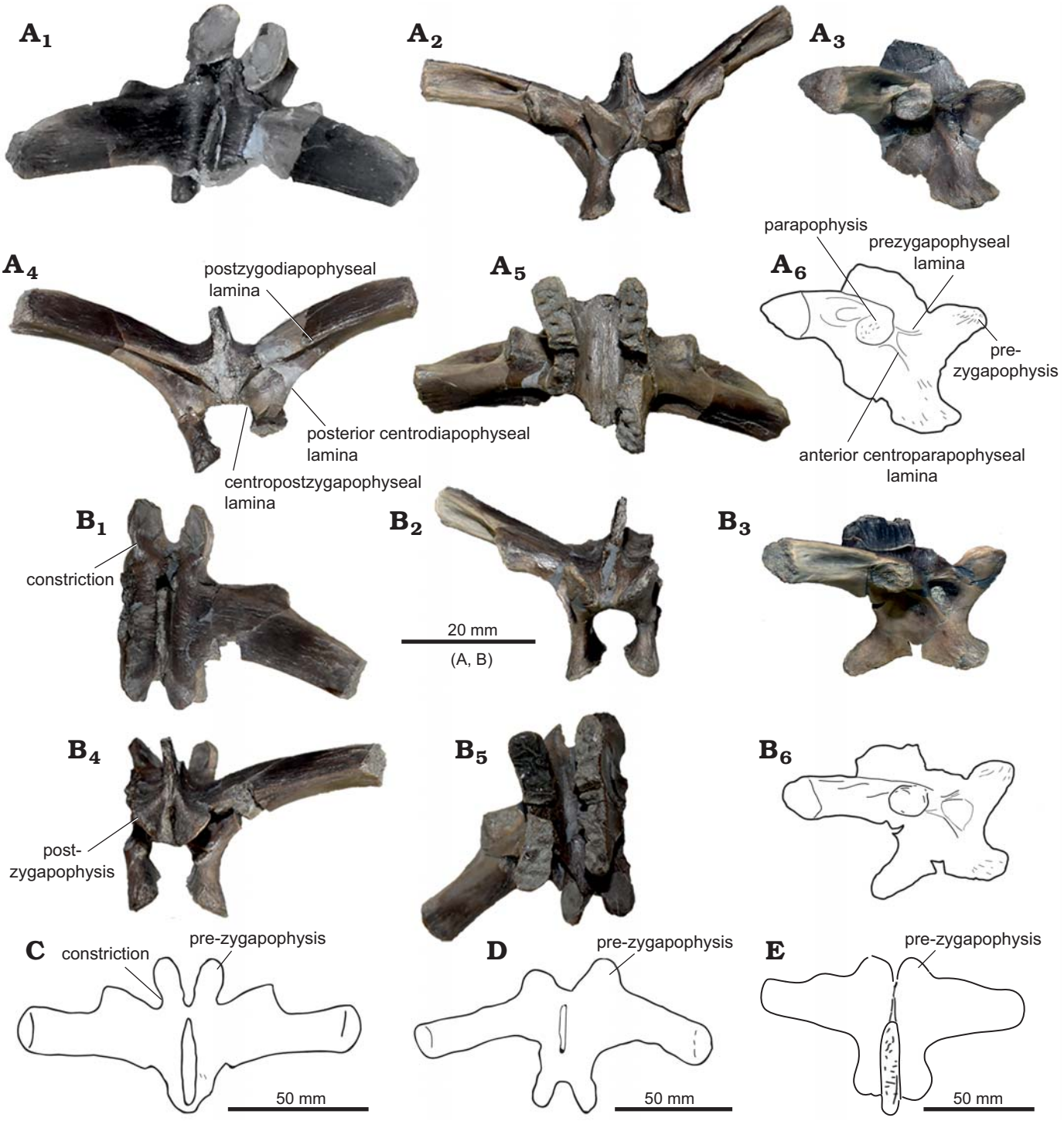

Fig. 3. Axial skeleton elements of Dryosauridae indet. (A, B) from the Lourinhã municipality, Portugal, Lourinhã Formation, Kimmeridgian–Tithonian compared with of *Dryosaurus altus* (C), *Camptosaurus* ("*Uteodon*") *aphanoecetes* (D), and *Mantellisaurus atherfieldensis* (E). Dorsal vertebrae: ML 2321a (**A**) and ML 2321b (**B**), in dorsal (A_1, B_1), anterior (A_2, B_2), lateral (A_3, A_6, B_3, B_6), posterior (A_4, B_4), and ventral (A_5, B_5) views. Dorsal neural arches: YPM 1876 (**C**), CM 11337 (**D**), IRSNB 1551 (**E**), in dorsal view.

the proximal epiphysis, has various fractures all along the shaft and was restored by epoxy resin, measuring 220 mm.

In the tibia ML 505 the proximal epiphysis exhibits a conspicuous cnemial crest, a well-developed fibular condyle, and a small inner condyle. The cnemial crest possesses a concave lateral edge and a convex medial edge. It is divided from the fibular condyle by a rounded surface (contrary to *Valdosaurus*, Barrett et al. 2011). The inner condyle points latero-posteriorly, being divided from the fibular condyle by a narrow sulcus. The mid-shaft section is sub triangular in cross section, being flattened laterally and sharp medially, having a conspicuous crest departing from the

distal-most part of the shaft (similar to the *Eousdryosaurus* holotype). The overall morphology of the shaft has been partially altered by the reconstruction process, therefore its taxonomical and systematical significance has to be considered cautiously. The distal epiphysis does not preserve any visible features, only the size of the two sub-equal malleoli.

In the tibia ML 2055 the proximal end is laterally compressed and fractured. The section of the mid-shaft is round (character 263: 1) with a small crest on the lateral side. The distal epiphysis preserves both malleoli and in anterior view they exhibit a highly rugose surface. A deep sulcus, extends for most of the surface area of the lateral malleolus. The medial malleolus possesses a less extensive notch, while the lateral malleolus is more elongated posterolaterally (character 264: 1). In distal view, the two malleoli are at right angles to one another.

Remarks.—Cranial skeleton: Parietal: Isolated parietals have not received much attention in literature, what hinders detailed comparisons. ML 1851 differs from *Othnielosaurus rex*, *Hypsilophodon foxii*, *Camptosaurus dispar*, and *Dryosaurus altus* in being sub triangular in general shape, having less anteriorly expanded lateral processes, a narrower sagittal crest, and proportionally longer posterior lateral processes (Gilmore 1909; Galton 1974, 1981; Norman et al. 2004). ML 1851 shows striking similarities with mature specimens of *Dysalotosaurus lettowvorbecki* (Janensch 1955; Galton 1981; Norman 2004), however, contrasting with the x-shaped morphology of the parietal present in immature specimens of the same species (Sobral et al. 2012). As in adults of *D. lettowvorbecki*, ML 1851 possesses a deeply arched lateral process which expands anteriorly, a W-shaped contact with the frontals, proportionately short posterior processes, and a wider sagittal crest (Hübner and Rauhut 2010; Sobral et al. 2012).

Dentary: The two crowns present in ML 768 shows the characteristic diamond shape typical of iguanodontian dinosaurs (Norman 2004; Galton 2006). The hook like denticles are typical of dryomorphan taxa such as *Dryosaurus altus*, *Dysalotosaurus lettowvorbecki*, *Iguanodon bernissartensis*, *Mantellisaurus atherfieldensis* (Norman 2004; Galton 2006). The number and position of primary and secondary ridges is extremely variable among species and even within the same tooth row, depending on the tooth position. ML 768 differs from the coeval ankylopollexians in the lack of a marked and mesially offset secondary ridge (Galton 2006). Instead, as in some specimens of *Dryosaurus* and *Dysalotosaurus* (Galton 1983, 2006; Carpenter and Galton 2018) the single main ridge is positioned towards the midline of the crown, slightly caudally offset.

Axial skeleton: *Neural arches*: The two isolated and disarticulated neural arches can be ascribed to Iguanodontia on the basis of stout transverse processes and zygapophyses inclined 45° with respect to one another (Norman 2004). Among iguanodontians, the constriction between the lobe of the prezygapophyses and the rest of the bony processes is not well-discussed in literature, but this character is present in Dryosauridae (Janensch 1955; Galton 1981). On the contrary, ankylopollexians show stout and bulky prezygapophyses, see for instance *Camptosaurus dispar*, *C. aphanoecetes*, *Mantellisaurus atherfieldensis*, and *Iguanodon bernissartensis* (Gilmore 1909; Norman 1980, 1986, 2004; Carpenter and Wilson 2008). Furthermore, the presence of anterior and posterior notches constituted by the abovementioned laminae, as seen in *Valdosaurus canaliculatus*, supports the attribution to Dryosauridae (Barrett et al. 2011). The unfused neural arch condition is common among dryosaurid individuals (Barrett et al. 2011; Barrett 2016; Hübner 2018) since even the largest individuals known so far did not attain complete skeletal maturity (Horner et al. 2009; Hübner 2012). This peculiar trait may explain why in this case and others reported (Barrett et al. 2011; Barrett 2016), isolated dorsal and cervical vertebral elements attributed to dryosaurids are often recovered disarticulated. On the contrary, vertebral elements of the caudal series fuse early in ontogeny (Hübner 2018) and therefore are usually recovered articulated (Galton 2009; Barrett et al. 2011; Barrett 2016; Hübner 2018).

Appendicular skeleton: *Femora*: The combination of an anteriorly bowed femoral shaft, the 4th trochanter proximally placed, and the medially relegated scar of Musculus caudofemoralis longus are diagnostic for Dryosauridae (Butler et al. 2008; Barrett et al. 2011; Escaso et al. 2014; Boyd 2015; Dieudonné et al. 2016). Nevertheless, ML 563 and ML 2055 differ from one another in some aspects. ML 563 is generally more gracile than ML 2055 in general proportions. This is herein interpreted as a difference in ontogenetic stages between the two individuals and therefore, as it is discussed in the next paragraphs, ML 563 probably represents a more immature individual than ML 2055. The difference in size is reflected in the different shape and depth of the extensor groove, which is greatly influenced by load. This is consistent from what is currently known in other dryosaurid populations, which show great intra-specific variation of the extensor groove according to the size (see, for instance, femora assigned to *Valdosaurus canaliculatus*, *Dryosaurus altus*, *Dysalotosaurus lettowvorbecki*, *Elrhazosaurus nigeriensis* in Galton 1981, 2009; Barrett et al. 2011; Hübner 2018). Another difference is the slightly different position of the scar of Musculus caudofemoralis longus. In ML 563 the position of the scar is well separated from the base of the 4th trochanter while in ML 2055 it extends further laterally to the base of the 4th trochanter, although still separate. Although it is generally assumed that a "widely separated scar of Musculus of caudofemoralis longus" is an unambiguous synapomorphy for Dryosauridae, in literature there are various examples of variation of this character even within the same population (Galton 1981). Furthermore, *Valdosaurus* and *Callovosaurus* specimens usually present the scar of the Musculus caudofemoralis longus connected to the base of the 4th trochanter (Ruiz-Omeñaca et al. 2006; Barrett et al. 2011) similarly to ML

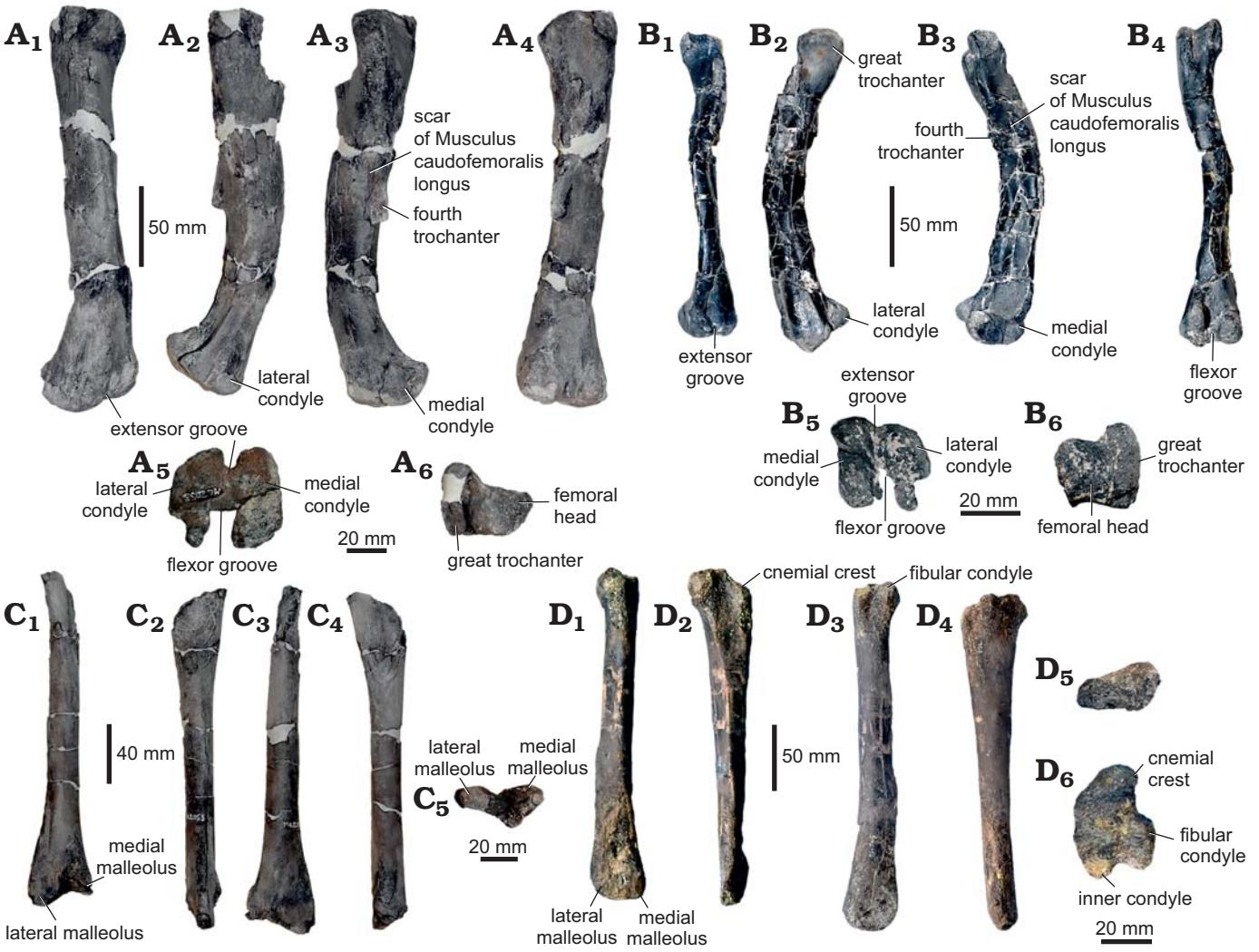

Fig. 4. Limb bones of Dryosauridae indet. from the Lourinhã municipality, Portugal, Lourinhã Formation, Kimmeridgian–Tithonian. **A**, **B**. Femur, ML 2055 (**A**), ML 563 (**B**), in anterior (A_1, B_1), lateral (A_2, B_2), medial (A_3, B_3), posterior (A_4, B_4), distal (A_5, B_5), and proximal (A_6, B_6) views. **C**, **D**. Tibia, ML 2055 associated to femur ML 2055 (**C**), ML 505 (**D**), in anterior (C_1, D_1), lateral (C_2, D_2), posterior (C_3, D_3), medial (C_4, D_4), proximal (D_5), and distal (C_5, D_6) views.

2055; while *Dryosaurus*, *Dysalotosaurus*, *Elrhazosaurus*, and *Eousdryosaurus* have it generally more widely separated (Galton 1981; Escaso et al. 2014) as in ML 563. Besides the inter-specific variation, an incipient intra-specific variation is present within populations of *Dryosaurus* and *Dysalotosaurus* (Galton 1981), where the insertion scar in some specimens is located more medially than others. As the extensor and flexor grooves, this character may also be influenced by size and varies during ontogeny as suggested by Hübner (2018). Therefore, the insertion scar of the Musculus caudofemoralis longus may be more plastic than previously thought and possibly related to ontogenetic development as well as with phylogeny.

The more mature specimen represented by ML 2055 resembles the overall morphology of an immature ankylopollexian as expected due to marked peramorphic conditions of basal ankylopollexians (i.e., camptosaurid) relative to dryosaurids (see Horner et al. 2009). Nevertheless, this possible attribution to Ankylopollexia is here considered unlikely for ML 2055 since the medial condyle is comparable in size to the lateral condyle, while in *Camptosaurus dispar* the medial condyle is described as "sensibly more robust" by Gilmore (1909) and the same condition is present in the Portuguese ankylopollexian species *Draconyx loureiroi*. Furthermore, the flexor groove is widely open, while in most specimens ascribed to the genus *Camptosaurus*, an incipient lateral expansion overhangs on the flexor groove (Galton and Powell 1980; Carpenter and Wilson 2008; Carpenter and Lamanna 2015).

Tibiae: The tibia ML 505, despite presenting a high degree of erosion, has many recognizable characters, which indicate dryosaurid affinities. In particular, ML 505 shares with *Dryosaurus*, *Dysalotosaurus*, and *Eousdryosaurus* a conspicuous fibular condyle placed in the midline of the proximal epiphysis and the presence of a wide groove between the posterior, inner, and fibular condyles (Janensch

1955; Galton 1981; Escaso et al. 2014). Ankylopollexians exhibit a different condition of the proximal epiphysis of the tibia in having the fibular condyle directed posteriorly (Norman 2004).

It should be noted that ML 505 has a triangular diaphyseal cross section, while in ML 2055 the cross section is tear-drop. This result is consistent both with incipient intra-specific variation as observed in *Dryosaurus* and *Dysalotosaurus* populations (Galton 1981).

Ankylopollexia Sereno, 1986

Ankylopollexia indet.

Figs. 5–8.

Material.—ML 2042, isolated, almost complete scapula from Praia da Peralta; ML 452, two associated vertebrae, ML 864, an isolated neural arch (not found in association with ML 452) from Praia de Porto das Barcas; ML 818, isolated dentary from Praia Vale Frades; ML 2206, isolated coracoids from Lourinhã coastline. All from Kimmeridgian–Tithonian of Lourinhã, Portugal.

Description.—*Cranial skeleton*: *Dentary* (Fig. 5A): The partial right dentary ML 818 is broken at both anterior and posterior extremities, measuring 150 mm in total length. The maximum depth is reached in the posterior extremity being 62 mm tall, while the anterior extremity is 49 mm tall. In general, the bone appears stout and compact, being heavily eroded towards the anterior-most part. The lateral surface is heavily eroded, although preservation of the coronoid process is fairly complete, missing just the dorsal-most end. The dorsal and ventral margins appear to be parallel to one another. The ventral surface is smooth, lacking a ventral flange (character 121: 0). The tooth row preserves ten, possibly eleven, distinguishable close-packed alveoli (character 136: 1). The tooth row, which ends medial to the coronoid process, is encased in a parapet-like shelf that is smoothly arched medially (character 122: 0). Two nutrient foramina are located on the marginal shelf of the tooth row (character 145: 0). Teeth are not preserved and the tooth-sockets do not show any interdental plates.

On the medial surface, dorsally to the Meckelian sulcus, a longitudinally striated surface extends almost to the anterior end of the specimen. Two other bones may have articulated against this surface: the splenial and the pre-articular. There is no difference in rugosity to distinguish these two areas.

On the lateral surface the coronoid process projects postero-laterally (characters 124: 1, 125: 1) with respect to the tooth-row and is inclined at about 30° to the horizontal. The contact with the surangular corresponds to the 4th alveolus counted from the coronoid process cranially, so it reaches further anteriorly than coronoid process.

Axial skeleton: *Dorsal vertebrae and neural arch* (Figs. 6, 7): ML 452 are two partially distorted and fractured associated vertebrae, while ML 864 is a broken and isolated neu-

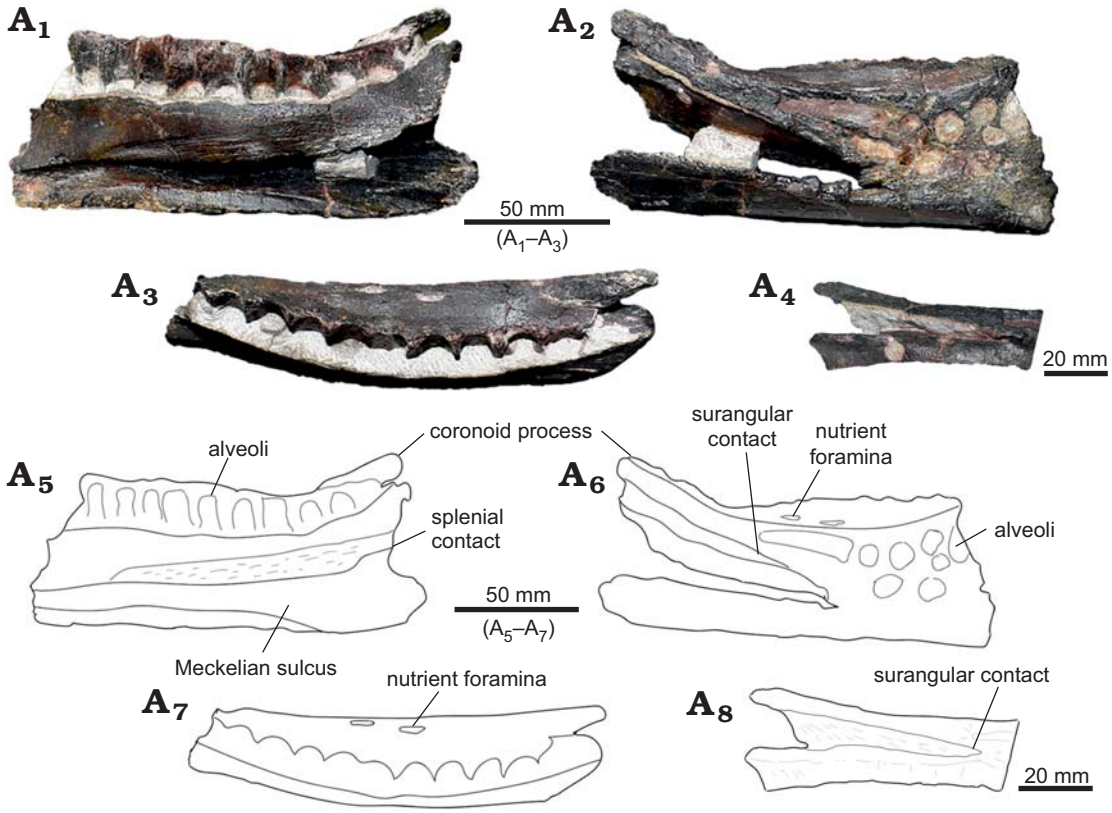

Fig. 5. Cranial material of Ankylopollexia indet. from the Lourinhã municipality, Portugal, Lourinhã Formation, Kimmeridgian–Tithonian. Dentary ML 818, in medial (A_1, A_5), lateral (A_2, A_6), and dorsal (A_3, A_7) views, detail of the dentary/surangular contact (A_4, A_8).

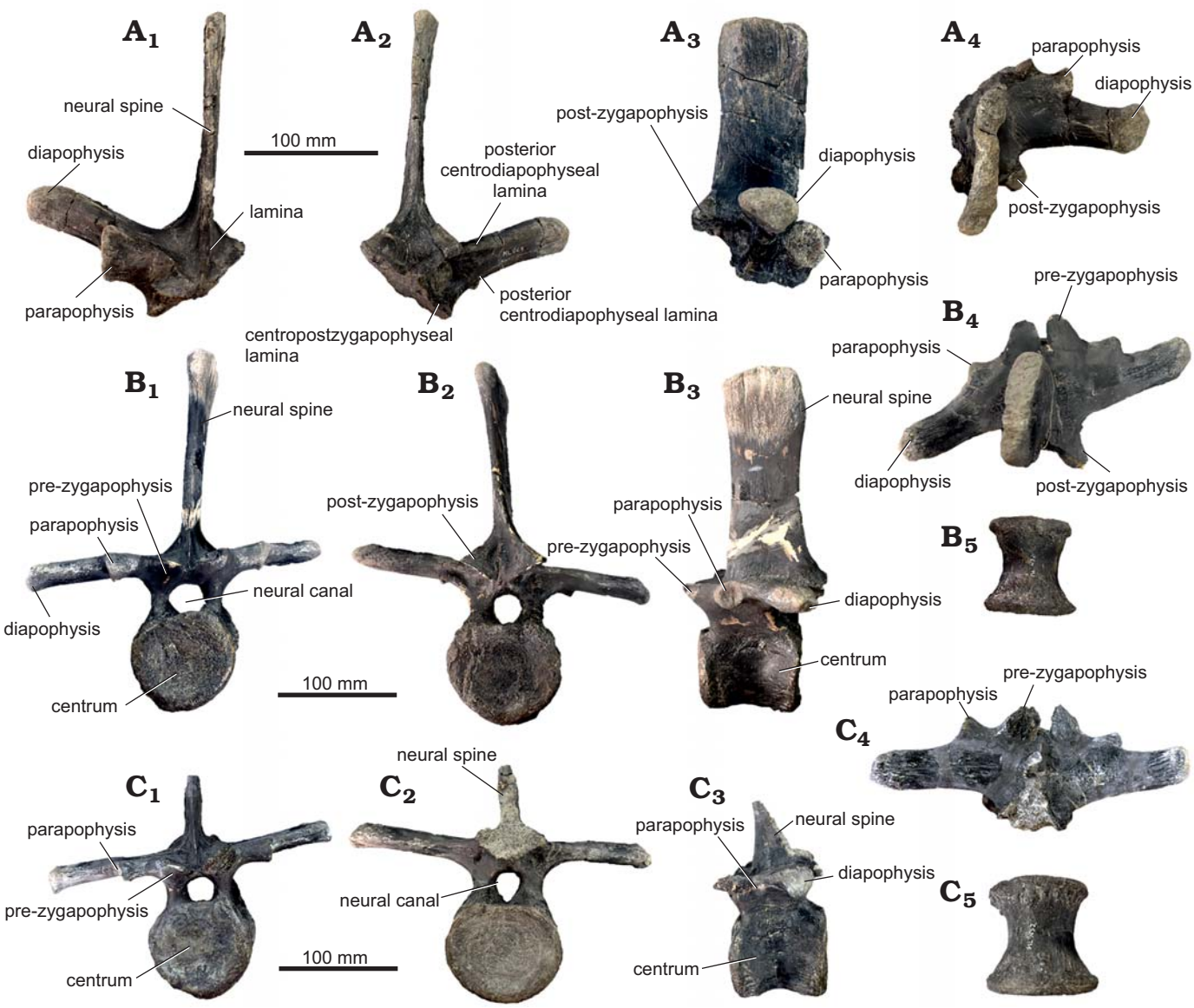

Fig. 6. Dorsal vertebrae Ankylopollexia indet. from the Lourinhã municipality, Portugal, Lourinhã Formation, Kimmeridgian–Tithonian. **A**. Partial neural arch, ML 864 in anterior (A_1), posterior (A_2), lateral (A_3), and dorsal (A_4) views. **B**, **C**. Dorsal vertebrae, ML 452a, complete (**B**) and ML 452b, incomplete (**C**) specimens, in anterior (B_1, C_1), posterior (B_2, C_2), lateral (B_3, C_3), dorsal (B_4, C_4), and ventral (digitally modified) (B_5, C_5) views.

ral arch, which preserves both postzygapophyses and one prezygapophysis. The two vertebrae ML 452 were found in association and therefore are interpreted to represent the same individual, while ML 864 is a second individual recovered from a different locality but comparable in size. Compared to the axial series of *Camptosaurus dispar* and *Mantellisaurus atherfieldensis*, ML 864 is most likely located at the 6–8th position of the dorsal series, while ML 452 are located after the 10th but before the 16th position of the dorsal series (Gilmore 1909; Norman 1986). The preserved centra are stout ranging 60–65 mm and consistently sub cylindrical in shape as in Ankylopollexia (Norman 2004), slightly amphicoelous with the anterior facet slightly bigger than the posterior (anterior facet height 60 mm, 65 mm; anterior width 65 mm, 73 mm; posterior height 60 mm, 73 mm; posterior width 75 mm, 70 mm). The slight amphicoelous condition indicates a close proximity to the sacrum. On the ventral surface, a slight constriction forms a smooth keel. The lateral surfaces of the centrum are longitudinally convex, showing the presence of small vascular foramina. The neural canal is fully open in both articulated vertebrae, being sub-circular in shape. Dorsally, two clearly distinguishable prezygapophysis are arranged in an angle of 45° with respect to one another, as in other iguanodontians (Norman 2004). Posterolateral to the prezygapophyses, the stout transverse processes originate, strongly inflecting dorsally in the partial neural arch. The associated vertebrae ML 452 show a strong lateroventral inflection on the left lateral side and a weaker dorsolateral inflection on the right side. The similar orientation of the transverse processes caused

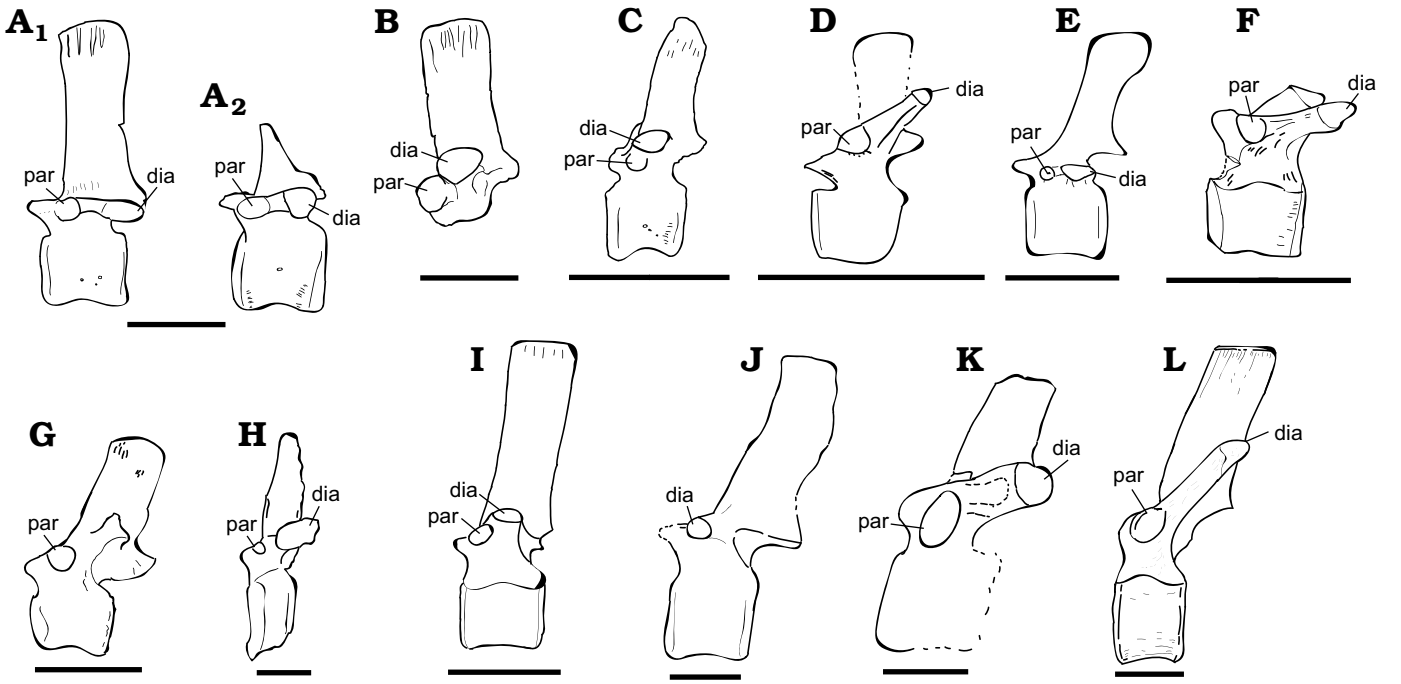

Fig. 7. Comparative dorsal vertebrae table of selected Ankylopollexians from the Late Jurassic and Early Cretaceous. **A**, **B**. Ankylopollexia indet. Lourinhã municipality, Portugal, Lourinhã Formation, Kimmeridgian–Tithonian. **A**. ML 452 in lateral view (A_1, A_2). **B**. ML 864 in right lateral view. **C**. "*Uteodon*" SHN.LPP 015 in left lateral view; Praia da corva, Torres Vedras Municipality, Portugal, Lourinhã Formation (Kimmeridgian–Tithonian) . **D**. "*Uteodon*" *aphanoecetes* CM 11337 in left lateral view; East end of Carnegie Quarry at Dinosaur National Monument, Uintah County, Utah (USA), Morrison Formation (Kimmeridgian–Tithonian). **E**. *Camptosaurus dispar* (unnumbered specimen) in left lateral view; Bone Cabin Quarry, Wyoming (USA), Morrison Formation (Kimmeridgian–Tithonian). **F**. "*Cumnoria*" *prestwichii* OUM. J.3303 in lateral view; Oxford, UK, Kimmeridge Clay Formation (Kimmeridgian–Tithonian). **G**. *Hippodraco scutodens* UMNH VP 20208 in left lateral view; Andrew's Site , Grand County, Utah; Upper Yellow Cat Memberof the Cedar Mountain Formation (upper Barremian–lowermost Aptian). **H**. *Iguanacolossus fortis* UMNH VP 20205 in right lateral view; Don's Ridge , Grand County, Utah, Lower Yellow Cat Member, Cedar Mountain Formation (?lower Barremian). **I**. *Mantellisaurus atherfieldensis* IRSNB 1551 in left lateral view; Isle of Wight, Wessex Formation (Barremian). **J**. *Barilium dawsoni* NHMUK R798 in left lateral view; Shornden, East Sussex, UK, Wadhurst Clay Formation (Valanginian). **K**. *Hypselospinus fittoni* NHMUK R604 in lateral view; Shornden Quarry, Hastings, UK, Wadhurst Clay Formation (Valanginian). **L**. *Iguanodon bernissartensis* IRSNB "Individu S" in left lateral view; Bernissart, Belgium, Sainte Barbe Clays Formation (Barremian). Abbreviations: dia, diapophysis; par, parapophysis. Scale bars 100 mm. Re-drawn from: C, Escaso 2014: fig. 6.5; D, Carpenter and Wilson 2008: fig. 11; E, Carpenter and Galton 2018: fig. 22D; F, Galton and Powell 1980: fig. 4; G, McDonald 2010b: fig. 27; H, McDonald 2010b: fig. 10; I, Norman 1980: fig. 37; J, Norman 2011: fig. 4; K, Norman 2015: fig. 22; L, Norman 1980: fig. 31).

by the same diagenetic alteration further supports the association of these two specimens. Similar cases are reported by Janensch (1955) describing bone beds of *Dysalotosaurs.* Nevertheless, it is here noted that in Ornithopoda, the transverse processes generally are not directed ventrally, therefore it is suggested the lateral left side has been affected by taphonomical processes more than the right one. The right transverse processes show an inclination which goes from weakly anterodorsal to nearly sub-horizontal, in the case of the most incomplete vertebrae of the pair. Comparing with other taxa (Gilmore 1909; Norman 1980, 1986; Carpenter and Wilson 2008; Carpenter and Lamanna 2015; Carpenter and Galton 2018) we note that this degree of inclination is consistent with undistorted specimens. Therefore, it is suggested that the right side has not been strongly affected by taphonomy, the inclination being different on the right lateral side a genuine character to discriminate the position of the vertebrae along the vertebral column. The different inclination of the transverse processes indicates that ML 864 is more cranially positioned than ML 452 vertebrae. This interpretation is corroborated also by the position of the parapophyses with respect to the diapophyses, being on two well separated planes in ML 864 and almost on the same one in ML 452 vertebrae, reflecting the general trend within Iguanodontia (Norman 2004). The neural spines rise immediately posterior to the prezygapophyses, with an anterior lamina encased by two lateral grooves, as in *Camptosaurus*, *Mantellisaurus atherfieldensis*, *Iguanodon bernissartensis*, and other ankylopollexians (Gilmore 1909; Norman 1980, 1986, 2004). In the most-complete vertebra of the sample, the neural spine is highly elevated with respect to the centrum as in other ankylopollexians, while dryosaurids have comparatively lower spines (Galton 1981). The overall shape of the neural spine is rectangular, a characteristic shared both by ML 452 and 864 individuals and different from the condition shown by *Camptosaurus dispar* and *C. aphanoecetes* (Gilmore 1909; Carpenter and Wilson 2008) but similar to that of *Mantellisaurus atherfieldensis.* Moderately deep grooves for the attachment of ossified tendons are visible on the apical-most part of the neural spine. Posteriorly, the postzygapophyses originate from the base of the neural spine.

Appendicular skeleton: *Coracoid* (Fig. 8A): The left coracoid ML 2206 is complete with the marginal sides slightly eroded. It is sub-rectangular in shape, bowed medio-laterally, and measures 130 mm in antero-posterior length and 108 mm in dorsoventral width. The dorsal margin is straight, while the ventral margin is deeply arched. The scapular surface is slightly concave and relegated to the dorsal-most part of the coracoid, while the glenoid surface is wider and slightly convex. Ventrally, the glenoid deflects abruptly, forming with the bowed ventral margin a conspicuous labrum. The coracoid foramen is dorsally located and totally enclosed on the lateral surface. On the medial surface, instead, it is open along the scapula-coracoid suture as in *Camptosaurus*, *Iguanodon*, *Mantellisaurus*, and derived iguanodontians (Gilmore 1909; Norman 1980, 1986). With derived iguanodontians it also shares the width/length ratio falling between 70–100% (Dieudonné et al. 2016). The sternal process is wide and broad, a plesiomorphic condition within Ornithopoda (Weishampel et al. 2003).

Scapula (Fig. 8B): ML 2042 is an incomplete and eroded scapula measuring 440 mm, missing the distal-most part of the blade and being partially eroded in the proximal end. The missing part is estimated to be not more than 10% of the total length of the whole scapular blade. The preserved dorsal and ventral margins appear to be parallel and progressively converging towards the distal part of the blade as seen in *Mantellisaurus atherfieldensis* and *Iguanodon bernissartensis* (Norman 1980, 1986), differently from the condition exhibited by *Camptosaurus dispar*, *C. aphanoecetes*, and *C. prestwichii* (Gilmore 1909; Carpenter and Wilson 2008; McDonald 2011; Carpenter and Lamanna 2015), which display a strong distal expansion towards the middle of the blade. The scapular blade is dorsoventrally bowed as in *Mantellisaurus atherfieldensis* and *Iguanodon bernissartensis* (Norman 1980, 1986). The proximal part flares gently, being concave on the lateral surface. The acromion process is slightly rounded and forwardly directed, the underlying coracoid suture is straight and ventrally deflects into the glenoid. Contrarily to *Camptosaurus dispar*, *C. aphanoecetes*, and *C. prestwichii* but similar to *Mantellisaurus atherfieldensis*, ML 2042 does not possess high protuberances corresponding to the acromion process and glenoid (Gilmore 1909; Norman 1980, 1986; Carpenter and Wilson 2008; McDonald 2011; Carpenter and Lamanna 2015).

Remarks.—Cranial skeleton: *Dentary*: ML 818 shares with other ankylopollexians, such as *Camptosaurus* spp., *Mantellisaurus atherfieldensis*, *Theiophytalia kerri*, *Iguanodon bernissartensis*, and *Kukufeldia tilgatensis*, parallel margins of the dentary, closed packed alveoli, and a highly emarginated parapet-like structure which constrains the tooth row (Gilmore 1909; Norman 1980, 1986; Brill and Carpenter 2006; McDonald et al. 2010a). These characters suggest an ankylopollexian affinity for ML 818. However, it differs from these taxa in having a more strongly inclined coronoid process, a condition shared with dryosaurids and *Tenontosaurus* spp. (Galton 1983; Thomas 2015). Furthermore, ML 818 has a dentary/surangular contact placed further anterior to the coronoid process as in basal taxa: *Hypsilophodon foxii*, *Dryosaurus altus*, *Dysalotosaurus lettowvorbecki*, and *Tenontosaurus* sp. (Galton 1974, 1983; Thomas 2015). This condition is different from other akylopollexians such as *Camptosaurus* spp., *Mantellisaurus atherfieldensis*, *Theiophytalia kerri*, *Iguanodon bernissartensis*, and *Kukufeldia tilgatensis* in which the dentary/surangular contact is placed on the same axis or immediately posterior to the coronoid process in a nearly perpendicular fashion (Gilmore 1909; Norman 2004; Brill and Carpenter 2006; McDonald et al. 2010a).

Axial skeleton: *Dorsal vertebrae and neural arch*: Ankylopollexians (and ornithopods in general) display a conservative axial skeleton during their evolutionary history, thus a taxonomic attribution of isolated material is problematic. The dorsal vertebrae ML 452 and the partial dorsal neural arch ML 864 are noteworthy in terms of size, they are bigger than most of the material recovered from the Lourinhã Formation, although it is comparable in size with *Camptosaurus* sp. dorsal vertebrae from the Morrison Formation, in particular USNM 4282 (Gilmore 1909) and the specimen discussed in Carpenter and Galton (2018: fig. 19G). The holotype of *Draconyx loureiroi* is a mature individual (Waskow and Mateus 2017), the caudal centra preserved ranges 46–58 mm in length, being sensibly smaller than the ones presented here (Mateus and Antunes 2001). The general size proportions also closely resemble the ones of *Mantellisaurus atherfieldensis* and *Hippodraco scutodens* (Norman 1986; McDonald et al. 2010b). Both ML 452 and ML 864 share with *Mantellisaurus atherfieldensis*, *Hippodraco scutodens*, *Iguanodon bernissartensis*, *Barilium dawsoni*, and *Hypselospinus fittoni* (Norman 1980, 1986, 2011, 2015; McDonald et al. 2010b) the antero-posterior stout proportions, the rectangular shape of the neural spine, and its ratio with respect to the centrum; while *Camptosaurus dispar* shows a paddle like structure towards the dorsal-most part of the spine and generally slender proportions (Fig. 7). Both ML 452 and ML 864 display a more developed neural spine with respect to the transverse processes as in *Mantellisaurus atherfieldensis*, *Iguanodon bernissartensis*, *Barilium dawsoni*, and *Hypselospinus fittoni* (Norman 1980, 1986, 2011, 2015); while in *Camptosaurus dispar* specimens it is less developed (Gilmore 1909; Norman 2004; Carpenter and Wilson 2008; Carpenter and Galton 2018). Herein, ML 452 and ML 864 are conservatively assigned to Ankylopollexia, although the antero-posterior extension of the neural spine and its rectangular shape, its development respect to centrum and transverse processes, suggests a possible affinity to Styracosterna.

Appendicular skeleton: *Coracoid*: The isolated coracoid ML 2206 possesses a short and broad sternal process, a typical basal condition within Ornithischia. It shares with ankylopollexians, basal ornithopods (non-dryomorphans) and neornithischians, a width/length ratio between 70–100%.

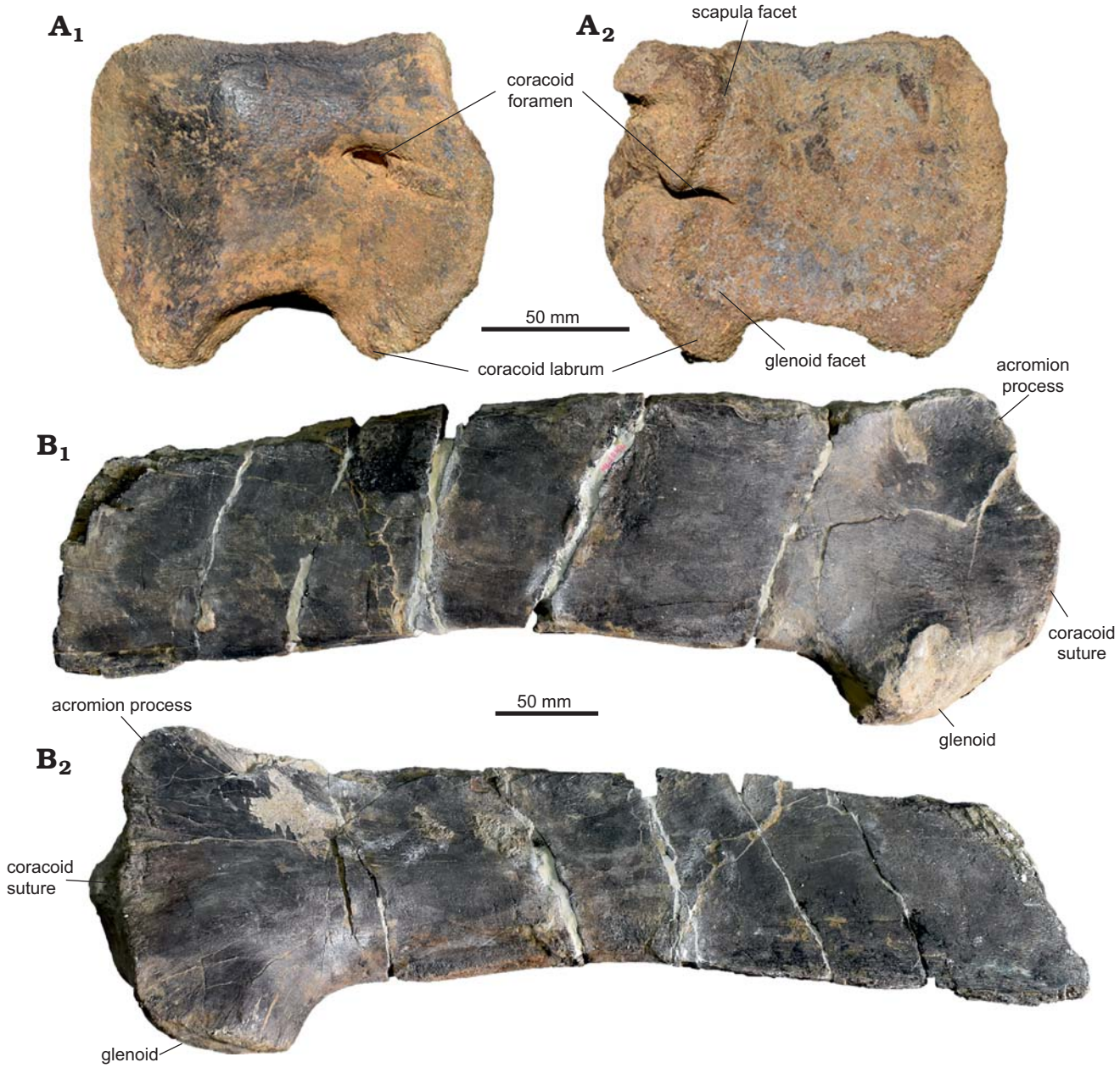

Fig. 8. Ankylopollexian appendicular skeleton from the Lourinhã municipality, Portugal, Lourinhã Formation, Kimmeridgian–Tithonian. Coracoid ML 2206 (**A**), scapula ML 2042 (**B**), in lateral (A_1, B_1) and medial (A_2, B_2) views.

It shares with dryomorphans, *Anabisetia saldivai*, and *Muttaburrasurus langdoni* an open coracoid foramen along the scapula-coracoid suture. The size of ML 2206 is greatly bigger than dryosaurids and other neornithischians (Galton 1974; Norman et al. 2004; Hübner 2018), while it is comparable with ankylopollexians (Gilmore 1909; Norman 1980, 1986; Carpenter and Wilson 2008; Carpenter and Lamanna 2015; Carpenter and Galton 2018). The coracoid ML 2206 does not present any distinguishable characters with respect to the variability shown by other ankylopollexians present in the Late Jurassic, such as *Camptosaurus* sp. (Dodson 1980; Carpenter and Wilson 2008; Carpenter and Lamanna 2015).

Scapula: ML 2042 shows characters which are widespread among Ankylopollexia, although they hint to more derived affinities. It is differentiated from *Camptosaurus dispar*, *C. prestwichii*, and dryosaurids in having the dorsal margin of the scapular blade convex and slender proportions of the proximal end with respect to the scapular blade. ML 2042 shares with *Barilium dawsoni*, *Hippodraco scutodens*, *Hypselospinus fittoni*, *Iguanacolossus fortis*, *Mantellisaurus atherfieldensis*, *Iguanodon bernissartensis*, and more derived Hadrosauriformes the general bowed outline of the scapular blade (Norman 1980, 1986, 2011, 2015; Horner et al. 2004; McDonald et al. 2010a, b). The scapular blade in *C. prestwichii*, *M. atherfieldensis*, *Hypselospinus fittoni*, and *I. bernissartensis* displays a concave proximal end (Norman 1980, 1986, 2015; Carpenter and Wilson 2008; McDonald 2011). The acromion process is rounded, differ-

ent from *C. dispar*, but similar to *C. aphanoecetes*, *M. atherfieldensis*, *Iguanodon bernissartensis*, and *Hypselospinus fittoni* (Gilmore 1909; Norman 1980, 1986, 2015; Carpenter and Wilson 2008; McDonald 2011). The ventral and dorsal margins, being sub-parallel towards the middle of the blade, resemble the condition seen in *M. atherfieldensis*, *I. bernissartensis*, and other derived styracosternans (Norman 2004) but differ from *C. dispar*, *C. aphanoecetes*, and *C. prestwichii* which have the ventral margin slightly diverging from the mid-blade or immediately distal to the mid-blade (Gilmore 1909; Carpenter and Wilson 2008; McDonald 2011). Carpenter and Lamanna (2015) lumped the once considered oldest styracosternan "*Uteodon*" *aphanoecetes* and "*Cumnoria*" *prestwichii* into the genus *Camptosaurus.* This lumping has great implications for the attribution of ML 2042 to Styracosterna, since some of the characters considered diagnostic present in the scapular blade (i.e., dorsal scapular margin convex, rounded acromion process) are now ambiguously widespread among Ankylopollexia. ML 2042 is here conservatively considered Ankylopollexia, although the presence of a dorsoventrally bow of the scapular blade, sub-parallel ventral and dorsal margins at mid-blade, and a generally rounded acromion indicates a possible attribution to Styracosterna.

Phylogenetic analysis

Six different phylogenetic analyses were carried out. First, the four most informative specimens, namely the isolated dentaries ML 768 and ML 818, and the limb bone elements ML 2055 and ML 563 alongside the holotype of *Eousdryosaurus nanohallucis* were included in the dataset of Dieudonné et al. (2016) in four independent analyses (A1–A4). Subsequently an analysis was performed using a dataset excluding the dentary ML 818, while including all the dryosaurid material and the *Eousdryosaurus nanohallucis* holotype (A5). Finally, a composite taxon consisting of the *Eousdryosaurus nanohallucis* holotype plus ML material attributable to dryosaurids was created in order to test the robustness of the previous phylogenetic results and to explore the possibility of assigning the ML material to *Eousdryosaurus nanohallucis* (A6). All the topologies recovered here do not differ substantially from the topology presented by Dieudonné et al. (2016). Ornithopoda here is recovered as the most inclusive clade including *Hypsilophodon foxii*, *Iguanodon bernissartensis*, their common ancestor and all its descendants. Contrary to Boyd (2015), Dieudonné et al. (2016) recovers *Parksosaurus warreni* in a more derived position than *H. foxii*, *Talenkauen santacrucensis*, and *Macrogryphosaurus gondwanicus*, but more basal with respect to *Anabisetia saldivai* and *Gasparinisaura cincosaltensis.* Iguanodontia is composed by *Anabisetia saldivai*, *Tenontosaurus* sp., *Muttaburrasaurus langdoni*, Rhabdodontidae, and Dryomorpha. The interrelationships between these taxa are recovered as the ones of Dieudonné et al. (2016), being *Tenontosaurus* sp. as sister to Dryomorpha. *Anabisetia* forms a clade with the node (*Tenontosaurus* sp. + Dryomorpha). *Muttaburrasaurus* is recovered as a sister to Rhabdodontidae.

In the topologies recovered here, all the specimens were recovered within Dryomorpha, either as basal dryomorphans, dryosaurids or ankylopollexians. The position of each specimen is here discussed in detail.

Analysis A1, Dieudonné et al. (2016) dataset + *E. nanohallucis* + ML 768 (Fig. 9A).—The dentary ML 768 was scored for 18 characters. The analysis resulted in 210 MPTs (CI 0.439, RI 0.654) of 766 steps. The strict consensus tree shows ML 768 recovered in a polytomy with *Dysalotosaurus lettowvorbecki*, *Dryosarus altus*, *Eousdryosaurus nanohallucis*, and Ankylopollexia. ML 768 is recovered as a dryomorphan based on the presence of a single synapomorphy: the primary ridge of the tooth-crown distally offset. Due to the fragmentary condition of the specimen and the lack of other diagnostic features, it is not possible to further resolve the position of ML 768 within Dryomorpha. Nevertheless, pruned trees show ML 768 either in a basal dryomorphan position or as Dryosauridae.

Analysis A2, Dieudonné et al. (2016) dataset + *E. nanohallucis* + ML 563 (Fig. 9B).—Isolated femur 563 was scored for ten characters. The analysis of ML 563 resulted in 126 MPTs (CI 0.439, RI 0.654) of 766 steps. The strict consensus tree shows ML563 recovered in a polytomy with *Dryosaurus altus*, *Dysalotosaurus lettowvorbecki*, and *Eousdryosaurus nanohallucis.* The inclusion of ML 563 is supported by the location of the scar of Musculus caudofemoralis longus being restricted to the medial part of the femoral shaft and the convex surface of the greater trochanter.

Analysis A3, Dieudonné et al. (2016) dataset + *E. nanohallucis* + ML 2055 (Fig. 9C).—Associated tibia and femur ML 2055 were scored for 14 characters. Similarly, the inclusion of ML 2055 is supported by the location of the scar of the Musculus caudifemoralis longus. However, ML 2055 differs from *Dryosaurus* and *Dysalotosaurus* in the shape of the 4th trochanter, which is blade-like in this specimen instead of being pendant as in other dryosaurids.

Analysis A4, Dieudonné et al. (2016) dataset + *E. nanohallucis* + ML 818 (Fig. 9D).—The partial dentary ML 818 was scored for six characters. The analysis of ML 818 resulted in 42 MPTs (CI 0.439, RI 0.649) of 766 steps. The strict consensus tree shows ML 818 recovered in a tricotomy with *Iguanodon bernissartensis* and *Camptosaurus dispar.* The inclusion of ML 818 within Ankylopollexia is supported by the close-packaging of the alveoli.

Analysis A5, Dieudonné et al. (**2016**) dataset + *E. nanohallucis* holotype + ML material (Fig. 10A).—The analysis of *Eousdryosaurus nanohallucis* holotype plus all the ML specimens produced 294 MPTs (CI 0.438, RI 0.653). *E. nanohallucis* holotype, ML specimens, *Dryosaurus altus* and *Dysalotosaurus lettowvorbecki* result in a polytomy

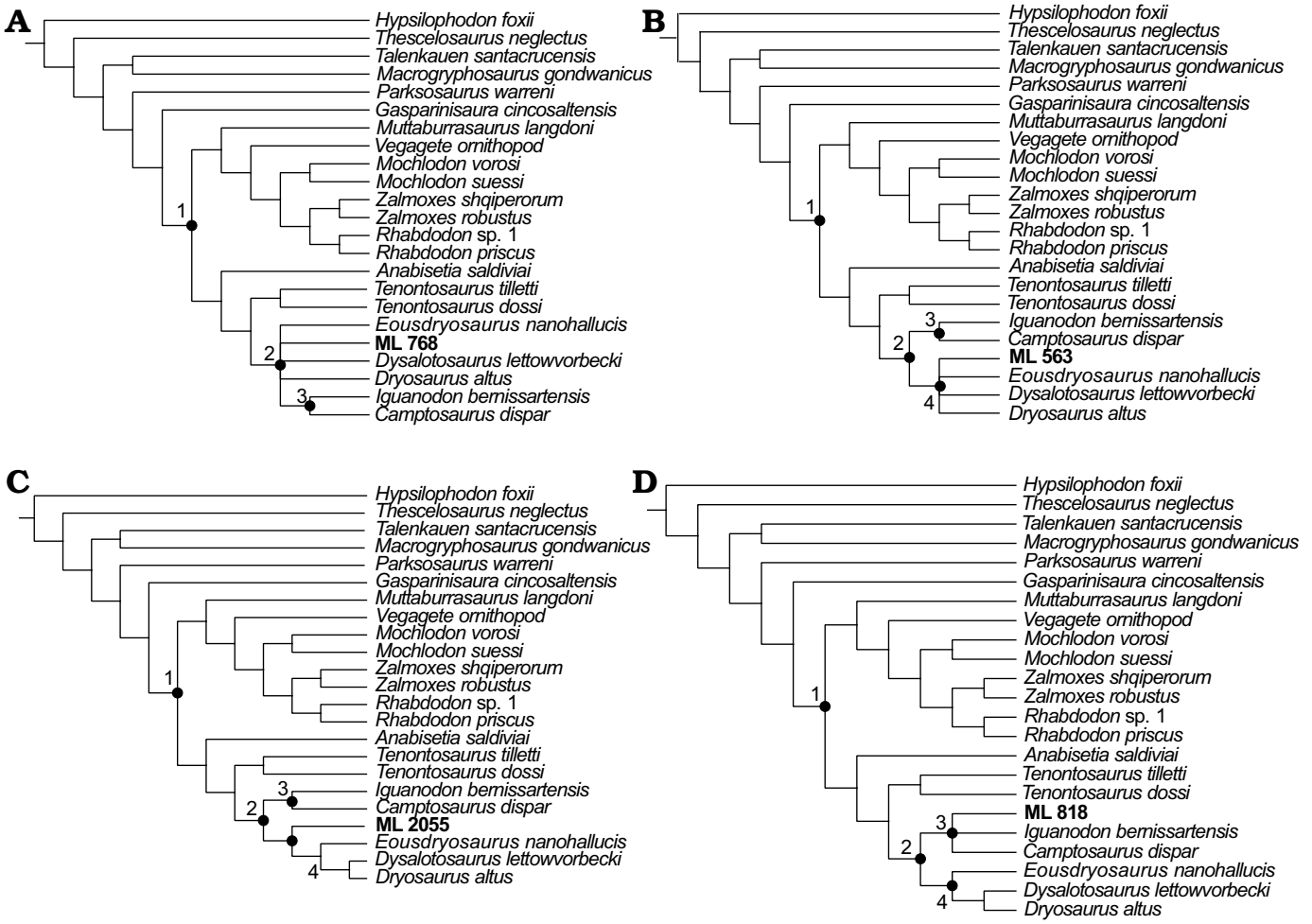

Fig. 9. Strict consensus tree, with the inclusion of ML 768 (**A**), ML 563 (**B**), ML 2055 (**C**), and ML 818 (**D**). Nodes: 1, Iguanodontia; 2, Dryomopha; 3, Ankylopollexia; 4, Dryosauridae.

within Dryomorpha in the strict consensus tree. The only synapomorphy supporting the inclusion of the material within Dryomorpha is, as in A1, the distally offset primary ridge of the tooth-crown. Despite the lack of resolution due to the fragmentation of ML 768, this result does not contradict the previous analyses. When ML 768 is removed a priori from the analysis, *E. nanohallucis* and ML material are better resolved. In particular, a topology is produced where ML 2055 is sister to the node composed by the unresolved polytomy of *Eousdrysaurus nanohallucis, Dryosaurus altus, Dysalotosaurus lettowvorbecki*, and ML 563. This result is consistent with the analyses A1–A3.

Analysis A6, Dieudonné et al. (2016) dataset + composite dryosaurid taxon (Fig. 10B).—The analysis which included the composite taxon formed by the ML specimens plus the *Eousdryosaurus nanohallucis* holotype, resulted in 42 MPTs (CI 0.438, RI 0.649). The strict consensus tree shows the composite taxon nested within Dryosauridae, as sister of *Dryosarus altus* + *Dysalotosaurus lettowvorbecki*. This affinity is consistent with previous analyses, but relationships within Dryosauridae have been shown to change easily in relation to sampling.

Principal Component Analysis.—To assess if the developmental state of the dryosaurid material from Portugal falls within the range of known dryosaurids, two separate Principal Component Analyses were carried out, including the shaft element proportions of the sample, one for the femora (Fig. 11D) and one for the tibiae (Fig. 11C). The resulting scatter plot shows clearly that in both cases, the material here examined (dots), falls within the range of variability of the *Dysalotosaurus lettowvorbecki* population.

In the case of the femora, Principal Component 1 (PC1) explains 84% percent of variance present in the sample and it is influenced positively equally by all the measured variables, with all the loading scores comprised between 0.25 and 0.35. According to Hammer and Harper (2008), when PC1 explains at least 80% of the variance present in the sample, in case of linear morphometric variables, it is safe to assume that PC1 represents the size variation of the sample. Therefore, PC1 is safely regarded as a proxy of size variation of the sample, taking into account the size of all measured elements. Principal Component 2 (PC2) explains 5.82 of the variance and contrary to PC1, two measured variables (22 and 30) are the ones which incise positively the most on PC2

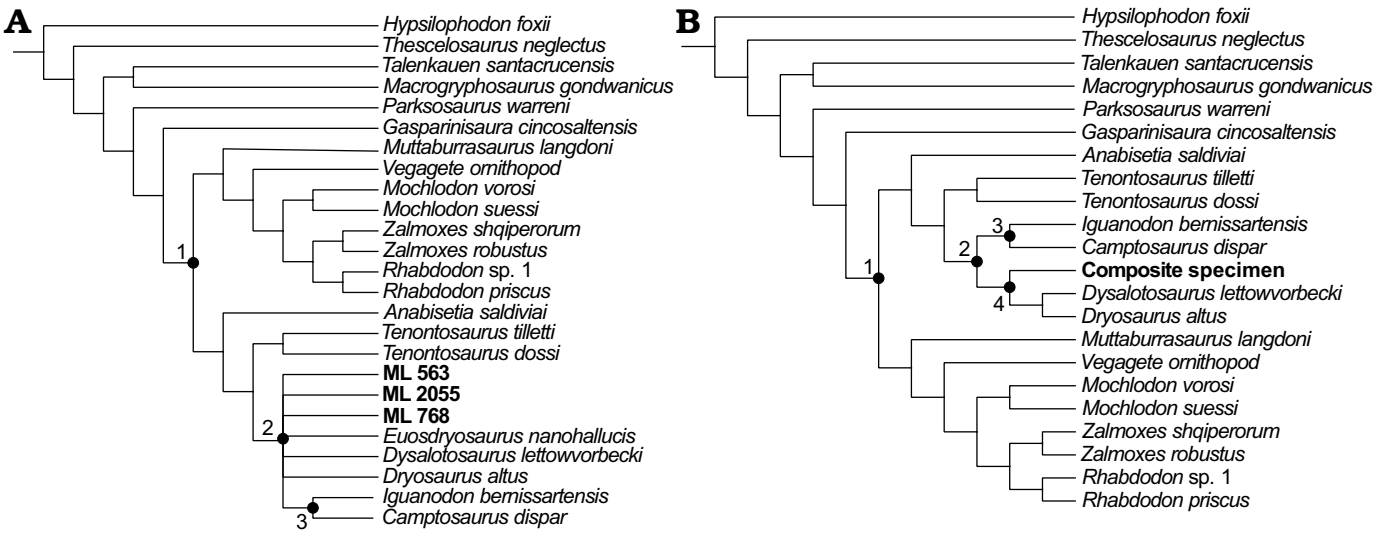

Fig. 10. Strict consensus trees of all the ML specimens + *Eousdryosaurus* holotype (**A**) and the composite of ML specimens and *Eousdryosaurus nanohallucis* holotype (**B**). Nodes: 1, Iguanodontia; 2, Dryomopha; 3, Ankylopollexia; 4, Dryosauridae.

(0.75 and 30, respectively). Variables 22 and 30 represent the variation in size of the flexor groove and the attachment surface for Musculus iliotibialis and all the flexor series. Notably, according to this analysis it appears that a larger size does not correspond with a bigger extensor groove.

In the case of the tibiae the PC1 explains 76–42% of the variance present in the sample and as in the case of the femora, it is influenced positively equally from all the measured variables, with loading scores ranging 0.09–0.30. Although PC1 approximates up to 80% of variance, the identity between size and PC1 is substantially weaker in this sample than in the previous case. Nevertheless, also in this case the PC1 reflects size taking into account all the measured anatomical part. PC2 explains 8.7% of variance present in the sample and it is mainly influenced positively by variables 4–12 and negatively by 13–19. The variables 4–12 refer to the size of the proximal end of the tibia, while the 13–19 refer to size of the distal ends of the tibia. According to the present analysis, there is a negative correlation between the two extremities of the tibial shaft. There is not a clear correlation between the overall size of the tibia and the size of the two ends.

Regression (RMA).—As in the case of PCA, two separate regressions were performed, one for the femora and one for the tibiae. In both cases, it was regressed PC1 values of every specimen, against the log of GM. As mentioned above, GM is a reliable proxy of absolute size, while PC1 scores besides the overall size of the specimen, reflect the variation in size of the measured elements. Since size is a reliable indicator of age in dryosaurids (Hübner 2012, 2018), the regression of PC1 against log GM produces therefore an ontogenetic growth series.

In the case of the femora (Fig. 11B), ML 2055 and ML 563 fit the linear model extrapolated. Strong correlation is found between size/age and skeletal elements measured ($r = 0.8997$, $p = 0.0001$). According to this model, ML 563 is nested within the most immature specimens considered, while ML 2055 is situated in a more intermediate position.

Similarly, in the case of the tibiae (Fig. 11A), ML 505 and ML 2055 fit the linear model extrapolated. Moderate correlation is found between age/size and skeletal elements measured ($r = 0.76199$, $p = 0.0001$). In the model produced, ML 505 and ML 2055 are located approximately within the same area, respectively slightly below and above the regression line, in an intermediate position with respect to the most immature individuals and the most mature ones. The close proximity of ML 505 and ML 2055 may indicate a similar ontogenetic stage.

Discussion

Dryosauridae.—Dryosaurid material includes cranial (ML 1851, ML 768), axial (ML 2321), and appendicualar (ML 2055, ML 563, ML 505) material. The attribution to Dryosauridae is supported by direct comparison and phylogenetic analysis, in some cases both. The isolated parietal ML 1851 is attributed to Dryosauridae on the basis of the sub triangular shape, posterior notch encased by the posterior walls of the lateral processes, and W contact with the frontals. As mentioned previously, these characters are nearly identical to the African dryosaurid species *Dysalotosaurus lettowvorbecki* (Janensch, 1955). In literature, the phylogenetic signal of this bone has been overlooked when it is not found in articulation with other bones of the braincase (Boyd 2015; Dieudonné et al. 2016). A deep revision of systematic and anatomy of basal ornithopods inter-relationships is beyond the reach of the present contribution; nevertheless, this is evidence of its potential significance even when found in isolation. Therefore, it is remarked here the necessity of including this character in future data matrices. The dentary

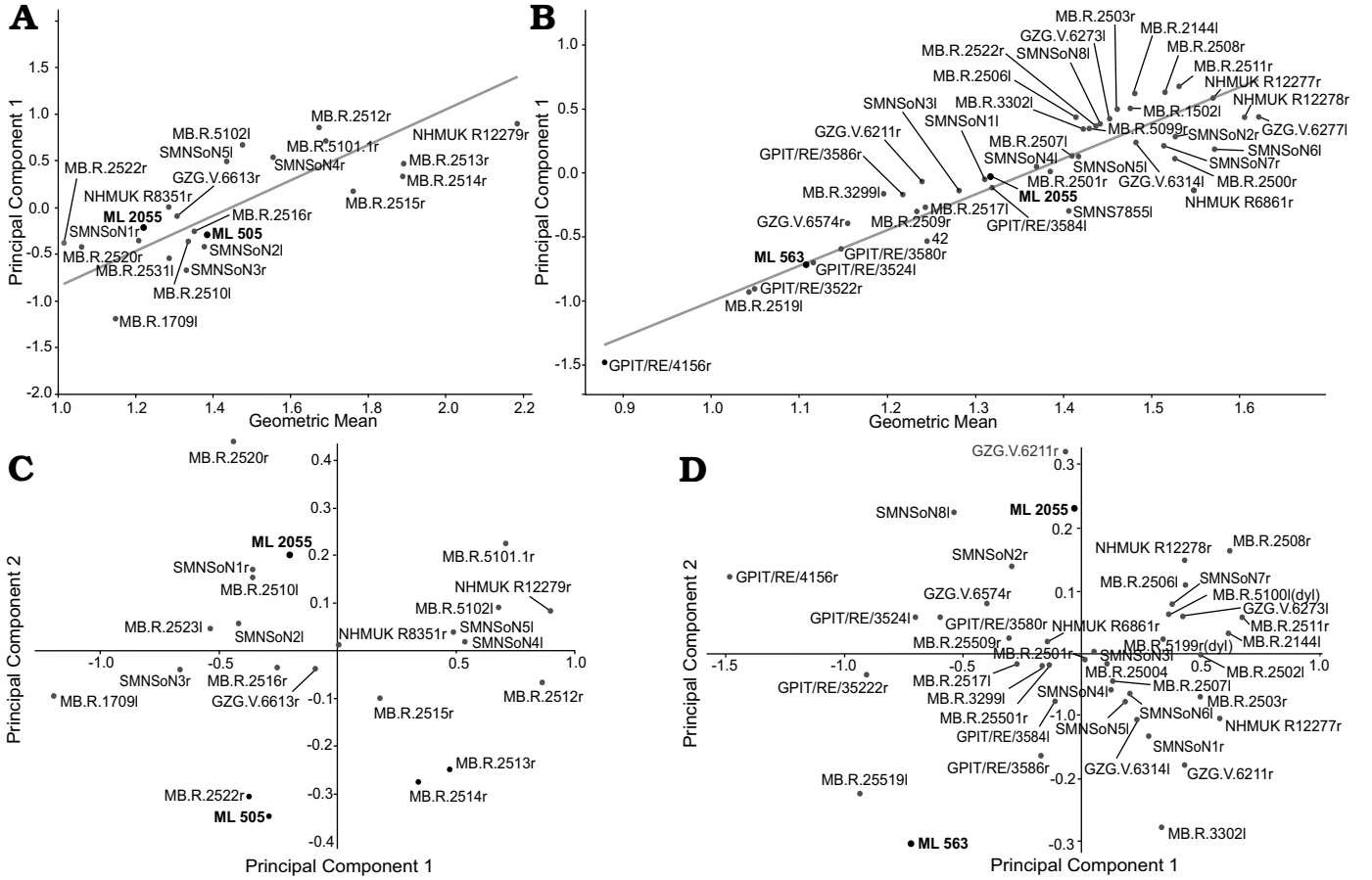

Fig. 11. Morphometric analysis results. Reduced Major Axis (RMA) for the tibiae (**A**) and femora (**B**). Principal Component Analysis (PCA) scatterplot of tibiae (**C**) and femora (**D**).

ML 768 is recovered within by the analysis 1 (A1) within Dryomorpha, on the basis of the primary ridge of the dentary tooth crown distally offset. Although the analysis could not better resolve ML 768, the position of the main ridge positioned towards the midline of the crown, a condition which is seen in *Dryosaurus altus* and *Dysalotosaurus lettowvobercki* (Janensch 1955; Galton 1981, 2006) indicates dryosaurid affinities for this specimen. Remarkably, this specimen is the only dentary ascribed so far to Dryosauridae from the Late Jurassic of Portugal. Therefore, since the lack of overlapping material with the Portuguese species and diagnostic features, ML 768 is considered as Dryosauridae indet. The two neural arches ML 2321 are here tentatively attributed to Dryosauridae on the basis of the arrangement of the posterior laminae, the short blade-like neural spine relatively to the transverse processes, as seen in *Valdosaurus canaliculatus*, *Dryosaurus altus*, and *Dysalotosaurus lettowvorbecki*. The rugose articulation between the neural arch and vertebral centrum, indicates a not completely fused condition. It is here interpreted as an immature ontogenetic stage for the individual represented by ML 2321, which is consistent regarding what is currently known about their palaeobiology. The limb elements ML 563 and ML 2055 are recovered by the analyses A3 and A4 (Fig. 9B, C) in Dryosauridae. This placement is supported by the proximally-located insertion scar for the Musculus caudofemoralis longus connected to the 4th trochanter, and relegated to the medial surface of the femoral shaft. These two specimens are recovered in two different positions by the two single analyses (Fig. 9). This result may be explained in terms of (i) differential preservation and completeness, (ii) different taxonomic attribution at species level or (iii) intra-specific variation. At the present time, there is no evidence to prefer one hypothesis to the other.

As discussed in previous sections, it may be argued that ML 2055 represents a juvenile ankylopollexian. The results of the direct comparison and phylogenetic analysis hints toward a more probable dryosaurid interpretation, but this possibility here is not entirely dismissed. In any case, ML 2055 is here referred consistently to Dryosauridae indet.

The tibia ML 505 is too fragmentary to test its affinities by phylogenetic analysis; therefore, it is here referred to Dryosauridae indet. on the basis of the deep sulcus between the inner and fibular condyle, and the conspicuous fibular condyle directed posteriorly.

The only dryosaurid ornithopod identified so far from the Lourinhã Formation is *Eousdryosaurus nanohallucis* (Escaso et al. 2014). The phylogenetic analysis carried out including ML 768, ML 563, ML 2055, and *E. nanohallucis* holotype (A5, Fig. 10A) indicates a close relationship between

ML material and *Eousdryosaurus nanohallucis*, supporting the previous analysis. The analysis which included the composite specimen (A6) further supports this interpretation. The composite specimens (Fig. 10B) are recovered in the same position as the *Eousdryosaurus nanohallucis* holotype as in previous analyses (Fig. 10D). Despite the close relationship of ML specimens to *Eousdryosaurus nanohallucis*, the aforementioned material cannot be ascribed to this species for the lack of overlapping material and diagnostic features.

Ankylopollexia.—Ankylopollexian are represented by cranial (ML 818), axial (ML 864, ML 452) and appendicular material (ML 2042, ML 2066). The dentary ML 818 is recovered within by the analysis 4 (A4) within Ankylopollexia on the basis of closely packed teeth. This interpretation is further corroborated by directly comparing ML 818 with other coeval taxa. *Draconyx loureiroi* (Mateus and Antunes 2001), represented only by post-cranial material, is the only ankylopollexian taxon recognized from the Late Jurassic of Portugal, although Escaso (2014) in his doctoral dissertation reported some specimens ascribed to Styracosterna, based on similarities with "*Uteodon*" *aphanoecetes*. Considering the recent taxonomic re-evaluation of the genus *Camptosaurus* by Carpenter and Lamanna (2015), who considered the following species valid: *C. dispar*, *C. aphanoecetes*, and *C. prestwichii* (the latter two were classified from McDonald [2011] as: "*Uteodon*" *aphanoecetes* and "*Cumnoria*" *prestwichii*), a great degree of intraspecific variability is implied to be present. Therefore, a taxonomic attribution and/or the institution of a new species based on isolated material, may be problematic, considering also the fact that Carpenter and Lamanna (2015) did not test their taxonomic hypothesis phylogenetically. This may lead also to a reconsideration of "styracosternan" material present from the Late Jurassic of Portugal. However, the presence of a (i) less inclined coronoid process of the dentary and (ii) the contact of the surangular placed further anterior than the coronoid process, distinguishes ML 818 from other Late Jurassic and Early Cretaceous ankylopollexians known. Giving the lack of overlapping material with respect to the holotype of *Draconyx loureiroi*, it is not possible to establish if ML 818 represents another individual of this species or an entirely new taxon. At the present time, it is here adopted a conservative approach and ML 818 is referred to Ankylopollexia without naming a new species or re-addressing the diagnosis of *Draconyx loureiroi*.

The isolated coracoid ML 2206 is attributed to Ankylopollexia on the basis of the ratio of width and length, which is consistent with other species. The isolated vertebral and appendicular elements ML 864, ML 452, and ML 2042 presents an unexpected morphology, being more similar to Early Cretaceous species rather than Late Jurassic forms. In particular, this material closely resembles the general anatomy of the styracosternan *Mantellisaurus atherfieldensis* and *Iguanodon bernissartensis* (Norman 1980, 1986). Therefore, an attribution to Styracosterna is plausible. However, as mentioned above, we conservatively refer these specimens to Ankylopollexia due to ambiguity in the diagnosis and identification of styracosternans from the Late Jurassic. In terms of size both the vertebrae and the scapula are comparable with already described *Camptosaurus* sp. specimens by Gilmore (1909). Therefore, the specimens herein described does not provide evidence for the gigantic size-class claimed by Mateus and Milan (2008) for the putative ornithopod tracks coming from the Lourinhã Formation. In any case, ML 864, ML 452, and ML 2042 indicate the presence of a previously unreported species of large size ankylopollexian, larger and possibly more derived than *Draconyx loureiroi*. Thus, it is here proposed that the diversity of large-sized iguanodontians from the Late Jurassic of Portugal, may have been overlooked.

Morphometric analysis.—The Principal Component Analysis suggests that the individuals represented by ML 563, ML 505, and ML 2055 fall within the range of variability of population of *Dysalotosaurus lettowvorbecki*. In the case of the femora, the increase in size is correlated with variation in the size of the flexor groove, although this variation appears chaotic and does not show any particular trend. This is consistent with the results of Hübner (2018), who found a positive allometric correlation with the extensor groove depth and the overall size of the femoral shaft, and no particular trend regarding the flexor groove. Nevertheless, the analysis found some specimens where larger shaft size corresponds to a smaller flexor groove. This is most probably a mathematical artifact due to the incompleteness of the specimens. As in the case of the femora, the PC1 is correlated with size increase and as in the case of the femurs, there is not a clear trend recognized in this analysis. The difference in the placement area of ML 505 and ML 2055 is probably due to the incompleteness of the specimen. Despite some mathematical ambiguity due to the fragmentation of the specimens here examined, the PCA indicates that the ML material falls within the range of variability of *Dysalotosaurus* population. The size increase has been proven to be a good proxy to estimate the ontogenetic stages in dryosaurids (Hübner 2018). The fact the ML specimens fit the variability of *Dysalotosaurus* suggests that, as may be expected, these closely related species underwent similar growth patterns. Since no fully mature specimen of *Dysalotosaurus* is currently known, this indicates that the ML material represents immature individuals. This interpretation is further supported by the regression of the Principal Component Analysis 1 against the log of the GM, which produced ontogenetic trajectories where the ML specimens fit the regression model. This is consistent with previous studies on the paleobiology of dryosaurids, showing evidence for high-growth rates and precocial sexual behaviour (Horner et al. 2009; Hübner 2012, 2018). This analysis has to be interpreted with caution, since the ML specimens do not represent the same species. Nevertheless, *Dysalotosaurus* is a good term of comparison due to (i) phylogenetic proximity

to the material herein presented and (ii) the high number of specimens recovered at various ontogenetic stages from the Tendaguru Formation (Janensch 1955; Galton 1981, 1983; Hübner 2012, 2018). The preliminary results presented here, may lead us to make the hypothesis that dryosaurids developed a common growth strategy. However, to test this hypothesis it is needed to broaden the sampling within Dryosauridae and to couple a histological approach with the morphometric one.

Paleobiogeographical and paleoecological implications for the Lourinhã ornithopod fauna.—Ornithopod dinosaurs are rare globally during the Late Jurassic, although major clades had already differentiated (Boyd 2015). As previously stated, for the Late Jurassic of Portugal, just *Draconyx loureiroi* and *Eousdryosaurus nanohallucis* are sufficiently well known to assess their affinity with a certain degree of accuracy. Thus, Ankylopollexia and Dryosauridae are the only two undisputed Ornithopoda clades recognized so far in the Late Jurassic of Portugal (Mateus and Antunes 2001; Antunes and Mateus 2003; Ortega et al. 2009; Escaso 2014). The putative "basal ornithopods" reported by Thulborn (1973), Galton (1980), and Martin and Krebs (2000) are in need of a systematic revision and may result with Neornithischia outside of Ornithopoda (Boyd 2015). This faunal assemblage closely resembles the one recovered in the Morrison Formation in general taxonomic composition, in having the ankylopollexians *Camptosarus dispar*, "*Uteodon*" (= *Camptosaurus*) *aphanoecetes*, the dryosaurids *Dryosaurus altus*, and the recently named *D. elderae* (Carpenter and Lamanna 2015; Carpenter and Galton 2018) the basal neornithischians *Othnielosaurus rex*, *Drinker nisti*, and *Nanosaurus agilis* (the latter being considered the senior synonym of the first two by Carpenter and Galton 2018), and the heterodontosaurid *Fruitadens haagarorum* (Butler et al. 2009). The higher diversity observed in the Morrison Formation in comparison to the Lusitanian Basin, may be explained in terms of preservation potential and outcrops extension. Nevertheless, considering the faunal interchange between the Lusitanian Basin and the Morrison Formation (Mateus 2006), the recovery of more complete specimens and the reappraisal of already discovered material will probably lead to assignment of the fragmentary Portuguese taxa to at least some of the aforementioned groups.

Other Late Jurassic faunas which display affinities with Portuguese specimens are the ones present within the Tendaguru Formation with the presence of *Dysalotosaurus lettowvorbecki* and the Kimmeridge Clay with the presence of "*Cumnoria*" (= *Camptosaurus*) *prestwichii* (Galton and Powell 1980; Mateus 2006). From Asturìas (Spain), fragmentary isolated remains tentatively referred to Camptosauridae and Dryosauridae have been reported (Ortega et al. 2006; Ruiz-Omeñaca et al. 2007), although the material is in need of revision. Most of the recent works addressing iguanodontians dispersal patterns do not take into account European, and in particular, Portuguese taxa (Boyd 2015; Xu et al. 2018). Due to the paucity of their record in Iberia (Canudo 2009), it is difficult to assess paleobiogeographic dispersal and vicariance patterns of ornithopods during the Late Jurassic. Recent phylogenetic hypothesis proposed for Gondwanan ornithopods (Bell et al. 2018; Herne et al. 2019; Rozadilla et al. 2019) recovered the clade Elesmaria composed by Australian, South American, and South African forms. The fossil record of Elesmarians ranges from Lower Cretaceous (Albian–Aptian) to Upper Cretaceous (Maastrichtian) (Herne et al. 2018, 2019; Rozadilla et al. 2019), and their phylogenetic position is recovered alternatively within Iguanodontia as sister of Dryomorpha, *Tenontosaurus* spp., and Rhabdodontidae (Rozadilla et al. 2019); or within Ornithopoda as sister of Iguanodontia (Herne et al. 2019). Despite the absence of a stable position of this clade within Ornithopoda, the stratigraphical and geographical distribution, suggests a split from Laurasian forms no later than the Middle Jurassic (Callovian), since the oldest form of derived dryomorphan were already differentiated (Ruiz-Omeñaca et al. 2006). The dispersal of ornithopods occurred probably before the complete split of Gondwana from Laurasia, and no later than the Middle-Late Jurassic as already proposed by Galton (1980) and further discussed by Fanti (2012). This biogeographical model has been validated for other dinosaur taxa, such as sauropods (Bindellini and Dal Sasso 2019; Mannion et al. 2019). Thus Portuguese fauna are pivotal to better understand this crucial moment in the evolutionary history of Ornithopoda.

Conclusions

Ornithopod material collected during the last 20 years of fieldwork by the Museu da Lourinhã was reviewed and described allowing better characterization of the Upper Jurassic fauna of the Lourinhã Formation.

Dryosaurid material includes remarkably rare cranial material (parietal, dentary), two cervico-dorsal neural arches, two femora, and two tibiae. All the material can be referred to Dryosauridae, with affinities to *Eousdryosaurus nanohallucis*. According to the morphometric analysis, the specimens represented by limb bones are immature individuals.

Ankylopollexia is represented by an isolated dentary, two isolated vertebrae and a neural arch, a scapula, and a coracoid. While it is not possible to assign the material to *Draconyx loureiroi*, isolated vertebral material and scapula provides evidence of at least another large-sized species of ankylopollexian from the Late Jurassic of Portugal. This species at the present time cannot be diagnosed, although it closely resembles stryacosternans present from the Early Cretaceous of Europe.

Despite its fragmentary condition and the paucity of the findings, Portuguese fauna should be considered in future analyses addressing the dispersal and vicariance patterns of Ornithopoda, due to its measurable impact in hypothesis testing.

Acknowledgements

We would like to thank the Museu da Lourinhã for providing specimens and facilities, especially: Carla-Alexandra Tomás, Bruno Pereira, Alexandre Audigane, and Carla Abreu. To Jesper Milàn (Geomuseum Faxe, Denmark) and Micael Martinho (ML) who found and prepared some of the specimens. We also thank the Sociedade de Historia Natural (Torres Vedras, Portugal) and in particular Bruno Camilo Silva and Joana Ferreira for providing access and assistance to the holotype of *Eousdryosaurus nanohallucis*. Cristiano Dal Sasso (Museu di Storia Naturale di Milano, Italy) provided comparison material and William Harcourt-Smith (American Museum of Natural History, New York City, USA) for helping with the morphometric analysis. We also thank all the members of the Lourinhã Paleoteam for their inputs in earlier versions of this manuscript. We thank the editor Stephen Brusatte (School of GeoSciences, The University of Edinburgh, Edinburgh, UK) and the reviewers Tom Hübner (Stiftung Schloss Friedenstein Gotha, Germany) and Peter Galton (University of Bridgeport, Connecticut, USA) for their comments, which greatly improved the quality of this manuscript. A special thanks to Vincent J. Cheng (ML) who proof-read this manuscript. FMR is supported by the Fundação para a Ciência e a Tecnologia, Portugal (Grant SFRH/BD/146230/2019). MMA is supported by the Fundação para a Ciência e a Tecnologia, Portugal (Grant SFRH/BPD/113130/2015). The research here presented has been supported by grants (GeoBioTec-NOVA and UIDB/04035/2020).

References

Antunes, M.T., and Mateus, O. 2003. Dinosaurs of Portugal. *Comptes Rendus Palevol* 2: 77–95.

Barrett, P.M. 2016. A new specimen of *Valdosaurus canaliculatus* (Ornithopoda: Dryosauridae) from the Lower Cretaceous of the Isle of Wight, England. *Memoirs of Museum Victoria* 74: 29–48.

Barrett, P.M., Butler, R.J., Twitchett, R.J., and Hutt, S. 2011. New material of *Valdosaurus canaliculatus* (Ornithischia: Ornithopoda) from the Lower Cretaceous of southern England. *Special Papers in Palaeontology* 86: 131–163.

Bell, P.R., Herne, M.C., Brougham, T., and Smith, E.T. 2018. Ornithopod diversity in the Griman Creek Formation (Cenomanian), New South Wales, Australia. *PeerJ 6*: e6008.

Bindellini, G. and Dal Sasso, C. 2019. Sauropod teeth from the Middle Jurassic of Madagascar, and the oldest record of Titanosauriformes. *Papers in Palaeontology* [published online, https://doi.org/10.1002/spp2.1282].

Boyd, C.A. 2015. The systematic relationships and biogeographic history of ornithischian dinosaurs. *PeerJ* 3: e1523.

Brill, K. and Carpenter, K. 2006. A description of a new ornithopod from the Lytle Member of the Purgatoire Formation (Lower Cretaceous) and a reassessment of the skull of *Camptosaurus*. *In*: K. Carpenter (ed.), *Horns and Beaks: Ceratopsian and Ornithopod Dinosaurs*, 49–67. Indiana University Press, Bloomington.

Butler, R.J., Galton, P.M., Porro, L.B., Chiappe, L.M., Henderson, D.M., and Erickson, G.M. 2009. Lower limits of ornithischian dinosaur body size inferred from a new Upper Jurassic heterodontosaurid from North America. *Proceedings of the Royal Society B: Biological Sciences* 277: 375–381.

Butler, R.J., Upchurch, P., and Norman, D.B. 2008. The phylogeny of the ornithischian dinosaurs. *Journal of Systematic Palaeontology* 6: 1–40.

Canudo, J.I. 2009. Dinosaurios ibéricos, final del Jurásico y la Formación Morrison. *Zubía* 27: 53–80.

Carpenter, K. and Galton, P. M. 2018. A photo documentation of bipedal ornithischian dinosaurs from the Upper Jurassic Morrison Formation, USA. *Geology of the Intermountain West* 5: 167–207.

Carpenter, K. and Lamanna, M.C. 2015. The braincase assigned to the ornithopod dinosaur *Uteodon* McDonald, 2011, reassigned to *Dryosaurus* Marsh, 1894: implications for iguanodontian morphology and taxonomy. *Annals of Carnegie Museum* 83 149–166.

Carpenter, K. and Wilson, Y. 2008. A new species of *Camptosaurus* (Ornithopoda: Dinosauria) from the Morrison Formation (Upper Jurassic) of Dinosaur National Monument, Utah, and a biomechanical analysis of its forelimb. *Annals of Carnegie Museum* 76: 227–264.

Dieudonné, P.-E., Tortosa, T., Fernández-Baldor, F.T., Canudo, J.I., and Díaz-Martínez, I. 2016. An unexpected early rhabdodontid from Europe (Lower Cretaceous of Salas de los Infantes, Burgos Province, Spain) and a re-examination of basal iguanodontian relationships. *PloS ONE* 11 (6): e0156251.

Dodson, P. 1980. Comparative osteology of the American ornithopods *Camptosaurus* and *Tenontosaurus*. *Memoirs of the Society of Geology, France* 139: 81–85.

Escaso, F. 2014. *Historia evolutiva de los Ornithischia (Dinosauria) del Jurásico Superior de Portugal*. 300 pp. Doctoral Dissertation, Universidad Autónoma de Madrid, Madrid.

Escaso, F., Ortega, F., Dantas, P., Malafaia, E., Silva, B., Gasulla, J.M., Mocho, P., Narváez, I., and Sanz, J.L. 2014. A new dryosaurid ornithopod (Dinosauria, Ornithischia) from the Late Jurassic of Portugal. *Journal of Vertebrate Paleontology* 34: 1102–1112.

Fanti, F. 2012. Cretaceous continental bridges, insularity, and vicariance in the southern hemisphere: which route did dinosaurs take? *In*: J.A. Talent (ed.), *Earth and Life*, 883–911. Springer, Dordrecht.

Foster, J. 2007. *Jurassic West: The Dinosaurs of the Morrison Formation and Their World*. 389 pp. Indiana University Press, Bloomington.

Foster, J. 2013. Ecological segregation of the Late Jurassic stegosaurian and iguanodontian dinosaurs of the Morrison Formation in North America: pronounced or subtle? *PalArch's Journal of Vertebrate Palaeontology* 10 (3): 1–11.

Galton, P.M. 1974. The ornithischian dinosaur *Hypsilophodon* from the Wealden of the Isle of Wight. *Bulletin of the British Museum (Natural History), Geology* 25: 1–152.

Galton, P.M. 1980. European Jurassic ornithopod dinosaurs of the families Hypsilophodontidae and Camptosauridae. *Neues Jahrbuch für Geologie und Paläontologie, Abhandlungen* 160: 73–95.

Galton, P.M. 1981. *Dryosaurus*, a hypsilophodontid dinosaur from the Upper Jurassic of North America and Africa postcranial skeleton. *Paläontologische Zeitschrift* 55: 271–312.

Galton, P.M. 1983. The cranial anatomy of *Dryosaurus*, a hypsilophodontid dinosaur from the Upper Jurassic of North America and East Africa, with a review of hypsilophodontids from the Upper Jurassic of North America. *Geologica et Palaeontologica* 17: 207–243.

Galton, P.M. 2006. Teeth of ornithischian dinosaurs (mostly Ornithopoda) from the Morrison Formation (Upper Jurassic) of Western United States. *In*: K. Carpenter (ed.), *Horns and Beaks. Ceratopsian and Ornithopod Dinosaurs*, 17–47. Indiana University Press, Bloomington.

Galton, P.M. 2009. Notes on Neocomian (Lower Cretaceous) ornithopod dinosaurs from England—*Hypsilophodon*, *Valdosaurus*, *"Camptosaurus"*, *"Iguanodon"*—and referred specimens from Romania and elsewhere. *Revue de Paléobiologie* 28: 211–273.

Galton, P.M. and Powell, H.P. 1980. The ornithischian dinosaur *Camptosaurus prestwichii* from the Upper Jurassic of England. *Palaeontology* 23: 411–443.

Gilmore, C.W. 1909. Osteology of the Jurassic reptile *Camptosaurus* with a revision of the species of the genus, and description of two new species. *Proceedings of the United States National Musuem* (36): 197–332.

Goloboff, P.A. and Catalano, S.A. 2016. TNT version 1.5, including a full implementation of phylogenetic morphometrics. *Cladistics* 32: 221–238.

Hammer, Ø. and Harper, D.A.T. 2008. *Paleontological Data Analysis*. 351 pp. John Wiley and Sons.

Hammer, Ø., Harper, D.A.T., and Ryan, P.D. 2001. PAST: Paleontological

Statistics Software Package for Education and Data Analysis. *Palaeontologia Electronica* 4 (1): 1–9.

Herne, M.C., Nair, J.P., Evans, A.R., and Tait, A.M. 2019. New small-bodied ornithopods (Dinosauria, Neornithischia) from the Early Cretaceous Wonthaggi Formation (Strzelecki Group) of the Australian-Antarctic rift system, with revision of *Qantassaurus intrepidus* Rich and Vickers-Rich, 1999. *Journal of Paleontology* 93 (3): 1–42.

Herne, M.C., Tait, A.M., Weisbecker, V., Hall, M., Nair, J.P., Cleeland, M., and Salisbury, S.W. 2018. A new small-bodied ornithopod (Dinosauria, Ornithischia) from a deep, high-energy Early Cretaceous river of the Australian-Antarctic rift system. *PeerJ* 5: e4113.

Hill, G. 1989. Distal alluvial fan sediments from the Upper Jurassic of Portugal: controls on their cyclicity and channel formation. *Journal of the Geological Society* 146: 539–555.

Horner, J.R., De Ricqlès, A., Padian, K., and Scheetz, R.D. 2009. Comparative long bone histology and growth of the "hypsilophodontid" dinosaurs *Orodromeus makelai*, *Dryosaurus altus*, and *Tenontosaurus tillettii* (Ornithischia: Euornithopoda). *Journal of Vertebrate Paleontology* 29: 734–747.

Horner, J.R., Weishampel, D.B., and Forster, C.A. 2004. Hadrosauridae. *In*: D.B. Weishampel, P. Dodson, and H. Osmólska (eds.), *The Dinosauria, 2nd Edition*, 438–463. University of California Press, Berkeley.

Hübner, T. 2012. Bone Histology in *Dysalotosaurus lettowvorbecki* (Ornithischia: Iguanodontia)—Variation, Growth, and Implications. *PLoS ONE* 7 (1): e29958.

Hübner, T. 2018. The postcranial ontogeny of *Dysalotosaurus lettowvorbecki* (Ornithischia: Iguanodontia) and implications for the evolution of ornithopod dinosaurs. *Palaeontographica A* 43–120.

Hübner, T. and Rauhut, O. W. M. 2010. A juvenile skull of *Dysalotosaurus lettowvorbecki* (Ornithischia: Iguanodontia), and implications for cranial ontogeny, phylogeny, and taxonomy in ornithopod dinosaurs. *Zoological Journal of the Linnean Society* 160: 366–396.

Janensch, W. 1955. Der Ornithopode *Dysalotosaurus* der Tendaguruschichten. *Palaeontographica-Supplementbände* 3: 105–176.

Klingenberg, C.P. 1996. Multivariate allometry. *In*: L.F. Marcus, M. Corti, A. Loy, G.J.P. Naylor, and D.E. Slice (eds.), *Advances in Morphometrics. NATO ASI Series (Series A: Life Sciences), Vol 284*, 23–49. Springer, Boston.

Madzia, D., Boyd, C.A., and Mazuch, M. 2018. A basal ornithopod dinosaur from the Cenomanian of the Czech Republic. *Journal of Systematic Palaeontology* 16: 967–979.

Mannion, P.D., Upchurch, P., Schwarz, D., and Wings, O. 2019. Taxonomic affinities of the putative titanosaurs from the Late Jurassic Tendaguru Formation of Tanzania: phylogenetic and biogeographic implications for eusauropod dinosaur evolution. *Zoological Journal of the Linnean Society* 185: 784–909.

Manuppella, G. 1998. Geologic data about the «Camadas de Alcobaça» (Upper Jurassic) North of Lourinhã, and facies variation. *Memórias da Academia de Ciências de Lisboa* 37: 17–24.

Manuppella, G., Antunes, M.T., Pais, J., Ramalho, M., and Rey, J. 1996. *Carta Geológica de Portugal 1:50000. Folha 30-A: Lourinhã.* Departamento de Geologico e Mineriro, Lisboa.

Marsh, O.C. 1881. Principal characters of American Jurassic dinosaurs. Part V. *American Journal of Science (Series 3)* 21: 417–423.

Martin, T. and Krebs, B. 2000. *Guimarota: a Jurassic Ecosystem*. 155 pp. Verlag Dr. Friedrich Pfeil, Münich.

Mateus, O. 2006. Late Jurassic dinosaurs from the Morrison Formation (USA), the Lourinhã and Alcobaça formations (Portugal), and the Tendaguru Beds (Tanzania): a comparison. *New Mexico Museum of Natural History and Science Bulletin* 36: 223–231.

Mateus, O. and Antunes, M. 2001. *Draconyx loureiroi*, a new camptosauridae (Dinosauria, Ornithopoda) from the Late Jurassic of Lourinhã, Portugal. *Annales de Paléontologie* 87: 61–73.

Mateus, O. and Milàn, J. 2008. Ichnological evidence for giant ornithopod dinosaurs in the Upper Jurassic Lourinhã Formation, Portugal. *Oryctos* 8: 47–52.

Mateus O. and Milàn, J. 2009. A diverse Upper Jurassic dinosaur ichnofauna from central-west Portugal. *Lethaia* 43: 245–257.

Mateus, O., Dinis, J., and Cunha, P.P. 2017. The Lourinhã Formation: The Upper Jurassic to lower most Cretaceous of the Lusitanian Basin, Portugal—landscapes where dinosaurs walked. *Ciências Da Terra–Earth Sciences Journal* 19: 75–97.

McDonald, A.T. 2011. The taxonomy of species assigned to *Camptosaurus* (Dinosauria: Ornithopoda). *Zootaxa* 2783: 52–68.

McDonald, A.T. 2012. Phylogeny of basal Iguanodonts (Dinosauria: Ornithischia): An update. *PLoS ONE* 7 (5): e36745.

McDonald, A.T., Barrett, P.M., and Chapman, S.D. 2010a. A new basal iguanodont (Dinosauria: Ornithischia) from the Wealden (Lower Cretaceous) of England. *Zootaxa* 2569: 1–43.

McDonald, A.T., Kirkland, J.I., DeBlieux, D.D., Madsen, S.K., Cavin, J., Milner, A.R., and Panzarin, L. 2010b. New basal iguanodonts from the Cedar Mountain Formation of Utah and the evolution of thumb-spiked dinosaurs. *PLoS One* 5 (11): e14075.

Milner, A.R. and Norman, D.B. 1984. The biogeography of advanced ornithopod dinosaurs (Archosauria: Ornithischia)—a cladistic-vicariance model. *In*: E. Reif and F. Westphal (eds.), *Third Symposium on Mesozoic Terrestrial Ecosystems, Short Papers*, 145–150. Attempto Verlag, Tubingen.

Norman, D.B. 1980. On the ornithischian dinosaur *Iguanodon bernissartensis* from the lower Lower Cretaceous of Bernissart (Belgium). *Memoir de l'Institut Royal des Sciences Naturelles de Belgique* 178: 1–105.

Norman, D.B. 1984. A systematic reappraisal of the reptile order Ornithischia. *Proceedings of the Third Symposium on Mesozoic Terrestrial Ecosystems*, 157–162. Attempto, Tübingen.

Norman, D.B. 1986. On the anatomy of *Iguanodon atherfieldensis* (Ornithischia: Ornithopoda). *Bulletin de l'Institut royal des Sciences naturelles de Belgique* 56: 281–372.

Norman, D.B. 2004. Basal Iguanodontia. *In*: D.B. Weishampel, P. Dodson, and H. Osmólska (eds.), *The Dinosauria*, 2nd edition, 413–437. University of California Press, Berkeley.

Norman, D.B. 2011. On the osteology of the lower Wealden (Valanginian) ornithopod *Barilium dawsoni* (Iguanodontia: Styracosterna). *Special Papers in Palaeontology* 86: 165–194.

Norman, D.B. 2015. On the history, osteology, and systematic position of the Wealden (Hastings group) dinosaur *Hypselospinus fittoni* (Iguanodontia: Styracosterna). *Zoological Journal of the Linnean Society* 173: 92–189.

Norman, D.B., Sues, H.-D., Witmer, L.M., and Coria, R.A. 2004. Basal Ornithopoda. *In*: D.B. Weishampel, P. Dodson, and H. Osmólska (eds.), *The Dinosauria*, 2nd edition, 393–412. University of California Press, Berkeley.

Ortega, F., Escaso, F., Gasulla, J.M., Dantas, P., and Sanz, J.L. 2006. Dinosaurios de la Península Ibérica. *Estudios geológicos* 62: 219–240.

Ortega, F., Malafaia, E., Escaso, F., Pérez García, A., and Dantas, P. 2009. Faunas de répteis do Jurássico Superior de Portugal. *Paleolusitana* 1: 43–56.

Owen, R. 1842. Report on British fossil reptiles. Part II. *In*: *Report of the Eleventh Meeting of the British Association for the Advancement of Science, Plymouth, England, July 1841*, 60–204. John Murray, London.

Rauhut, O. W. 2001. Herbivorous dinosaurs from the Late Jurassic (Kimmeridgian) of Guimarota, Portugal. *Proceedings of the Geologists' Association* 112: 275–283.

Rozadilla, S., Agnolín, F.L., and Novas, F.E. 2019. Osteology of the Patagonian ornithopod *Talenkauen santacrucensis* (Dinosauria, Ornithischia). *Journal of Systematic Palaeontology* 17: 2043–2089.

Ruiz-Omeñaca, J.I., Piñuela, L., and García Ramos, J.C. 2007. Una vértebra de un pequeño ornitópodo (Dinosauria: Ornithischia) del Kimmeridgiense (Formación Lastres) de Tazones (Villaviciosa, Asturias). *Geogaceta* 42: 83–86.

Ruiz-Omeñaca, J.I., Pereda Suberbiola, X., and Galton, P.M. 2006. *Callovosaurus leedsi*, the earliest dryosaurid dinosaur (Ornithischia: Eu-

ornithopoda) from the Middle Jurassic of England. *In*: K. Carpeneter (ed.), *Horns and Beaks: Ceratopsian and Ornithopod Dinosaurs*, 3–16. Indiana University Press, Bloomington.

Seeley, H.G. 1887. On the classification of the fossil animals commonly called Dinosauria. *Proceedings of the Royal Society of London* 43: 165–171.

Sereno, P.C. 1984. The phylogeny of the Ornithischia: a reappraisal. *In*: E. Reif and F. Westphal (eds.), *Third Symposium on Mesozoic Terrestrial Ecosystems, Short Papers*, 219–226. Attempto Verlag, Tubingen.

Sereno, P.C. 1986. Phylogeny of the bird-hipped dinosaurs (Order Ornithischia). *National Geographic Research* 2: 234–256.

Sobral, G., Hipsley, C.A., and Müller, J. 2012. Braincase redescription of *Dysalotosaurus lettowvorbecki* (Dinosauria, Ornithopoda) based on computed tomography. *Journal of Vertebrate Paleontology* 32: 1090–1102.

Taylor, A.M., Gowland, S., Leary, S., Keogh, K.J., and Martinius, A.W. 2014. Stratigraphical correlation of the Late Jurassic Lourinhã Formation in the Consolação Sub-basin (Lusitanian Basin), Portugal. *Geological Journal* 49: 143–162.

Thomas, D.A. 2015. The cranial anatomy of *Tenontosaurus tilletti* Ostrom, 1970 (Dinosauria, Ornithopoda). *Palaeontologia Electronica* 18 (2): 1–99.

Thulborn, R.A. 1973. Teeth of ornithischian dinosaurs from the Upper Jurassic of Portugal. Contribuiçao para o Conhecimento da Fauna do Kimeridgiano da Mina de Lignito Guimarota (Leiria, Portugal) III Parte, VI. *Memórias dos Serviços geológicos de Portugal (nova Sér.)* 22: 89–134.

Waskow, K. and Mateus, O. 2017. Dorsal rib histology of dinosaurs and a crocodylomorph from western Portugal: skeletochronological implications on age determination and life history traits. *Comptes Rendus Palevol* 16: 425–439.

Weishampel, D.B. 1984. Evolution of jaw mechanisms in ornithopod dinosaurs. *Advances in Anatomy, Embryology, and Cell Biology* 87: 1–109.

Weishampel, D.B., Jianu, C.-M., Csiki, Z., and Norman, D.B. 2003. Osteology and phylogeny of *Zalmoxes*, an unusual euornithopod dinosaur from the latest Cretaceous of Romania. *Journal of Systematic Palaeontology* 1: 65–123.

Xu, X., Tan, Q., Gao, Y., Bao, Z., Yin, Z., Guo, B., Wang, J., Tan, L., Zhang, Y., and Xing, H. 2018. A large-sized basal ankylopollexian from East Asia, shedding light on early biogeographic history of Iguanodontia. *Science Bulletin* 63: 556–563.